

Appendix E

<p style="text-align: center;"><b>NUCLEAR WASTE MANAGEMENT PROGRAM</b></p> <p><small>Sandia National Laboratories</small></p>	<h2 style="margin: 0;">Design Document Criteria Form</h2>	<p><b>Form Number: NP 19-1-4</b></p> <p><b>Page 1 of 1</b></p>
<p>1. <b>Software Name:</b> <u>DRSPALL</u></p> <p>2. <b>Software Version:</b> <u>1.00</u></p> <p>3. <b>Document Version:</b> <u>1.10</u></p> <p>4. <b>ERMS #:</b> <u>529878</u></p>		
<p><small>Prior to sign-off of the DD, all items shall be appropriately addressed by the code sponsor so that "Yes" may be checked. Include this form as part of the DD.</small></p>		
<p><b>Are the following appropriately defined and documented in the DD?</b></p> <p>5. Major Software Components <span style="float: right;"><input checked="" type="checkbox"/> Yes</span></p> <p>6. Technical description of the software with respect to: theoretical basis, embodied mathematical model, major control flow, control logic, and data structures <span style="float: right;"><input checked="" type="checkbox"/> Yes</span></p> <p>7. Allowable or Prescribed Ranges for Inputs and Outputs <span style="float: right;"><input checked="" type="checkbox"/> Yes</span></p> <p>8. Verifiability: Is the design verifiable through testing or other means? <span style="float: right;"><input checked="" type="checkbox"/> Yes</span></p> <p>9. Consistency and Traceability: Is the design consistent with and traceable to the software's requirements? <span style="float: right;"><input checked="" type="checkbox"/> Yes</span></p> <p>10. Technical Feasibility: Is the design technically feasible? <span style="float: right;"><input checked="" type="checkbox"/> Yes</span></p> <p>11. Implementation: Is the design presented in sufficient detail to allow for implementation as computer software? <span style="float: right;"><input checked="" type="checkbox"/> Yes</span></p>		
<p><u>DAVID LOED</u> 12. <b>Code Team/Sponsor</b> <small>(print)</small></p>	<p><u>David L Loed</u> Signature</p>	<p><u>9/9/2003</u> Date</p>
<p><u>Clifford Hansen</u> 13. <b>Technical Reviewer</b> <small>(print)</small></p>	<p><u>Clifford Hansen</u> Signature</p>	<p><u>9/9/2003</u> Date</p>
<p><u>David Kessel</u> 14. <b>Responsible Manager</b> <small>(print)</small></p>	<p><u>David Kessel</u> Signature</p>	<p><u>9/9/03</u> Date</p>
<p><u>Jennifer Long</u> 15. <b>SCM Coordinator</b> <small>(print)</small></p>	<p><u>Jennifer Long</u> Signature</p>	<p><u>9/9/03</u> Date</p>

**Key for check boxes above:**

Check **Yes** for each item reviewed and found acceptable

Information Only

**WIPP PA  
DESIGN DOCUMENT  
for  
DRSPALL Version 1.00**

**Document Version 1.10  
ERMS# 529878  
September, 2003**

**Information Only**

## Table of Contents

1	Introduction .....	5
1.1	Software Identifier .....	5
1.2	Points of Contact .....	5
1.3	Description .....	5
2	Major Code Components.....	7
3	Theoretical Basis .....	8
3.1	Wellbore Flow Prior to Penetration.....	11
3.2	Repository Flow Prior to Penetration.....	11
3.3	Coupling of Wellbore and Repository Flow Prior to Penetration.....	12
3.4	Wellbore Flow After Penetration .....	13
3.5	Repository Flow After Penetration.....	14
3.6	Coupling of Wellbore and Repository After Penetration.....	14
3.7	Preparation for Verification and Validation Testing.....	14
4	Mathematical Model.....	15
4.1	Wellbore Equations .....	15
4.1.1	Wellbore friction factor .....	17
4.1.2	Viscosity of wellbore slurry .....	18
4.1.3	Wellbore boundary conditions .....	19
4.2	Wellbore-Repository Coupling Equations Prior to Penetration.....	19
4.3	Repository Equations .....	22
4.3.1	Non-Darcy Flow.....	23
4.3.2	Elastic Response and Failure.....	25
4.3.3	Fluidization.....	26
4.3.4	Repository Boundary Conditions.....	27
4.3.5	Implementation of conceptual submodels in DRSPALL.....	28
4.4	Wellbore-Repository Coupling Equations Following Penetration.....	29
4.4.1	Geometry-Dependent Equivalent Drilled Radius.....	30
4.5	Numerical Method – Wellbore.....	31
4.6	Numerical Method – Repository .....	33
4.6.1	Boundary Conditions.....	34
4.6.2	Repository Stress State.....	34
4.7	Numerical Method – Coupling.....	34
4.8	Time Step Determination .....	35
5	Flow Chart with Functional Requirements Map .....	37
5.1	Call Tree With Subroutine Descriptions .....	42
6	Data Structures (I/O) .....	44
6.1	Input Files.....	44
6.1.1	Input Control and Parameter File .....	44
6.1.2	Input CDB File.....	45
6.2	Output Files .....	45
6.2.1	Output Text Files.....	45
6.2.2	CDB Output File .....	45
6.3	FORTRAN 90 Global Variables Modules .....	46
7	Parameter Ranges .....	52
8	Test Case Control Logic.....	55

- 8.1 Porous Flow Test Problem ..... 56
  - 8.1.1 Constant pressure inner boundary ..... 56
  - 8.1.2 Effective bit diameter ..... 56
  - 8.1.3 Special output and *dimensionless variables* ..... 57
- 8.2 Coalbed Methane Field Scale Test Case ..... 58
- 8.3 Internal Logic Checks Test Problem ..... 58
- 8.4 Wellbore Hydraulics Model Test Case ..... 58
  - 8.4.1 Lower boundary condition ..... 59
- 9 References ..... 60
- 10 Appendix A: Functional Requirements ..... 62
  - 10.1 External Interface Requirements ..... 62

### List of Figures

<b>Figure 2-1.</b> Flow chart of major code components.....	7
<b>Figure 3-1.</b> Schematic diagram of the flow geometry prior to repository penetration.....	9
<b>Figure 3-2.</b> Schematic diagram of the flow geometry after repository penetration. Spherical case is shown. ....	10
<b>Figure 3-3.</b> Effective wellbore flow geometry before bit penetration.....	11
<b>Figure 4-1.</b> Drawing of typical radial effective stress curve in DRSPALL repository domain at some time during drill penetration. ....	28
<b>Figure 4-2</b> Finite difference zoning for wellbore. ....	31
<b>Figure 5-1.</b> Flow Chart for Program DRSPALL.....	38
<b>Figure 5-2.</b> Flow Chart for Subroutine RunLoop.....	39
<b>Figure 5-3.</b> Flow Charts for Subroutines CalculateWellBoreFlow.....	40
<b>Figure 5-4.</b> Flow Chart for Subroutine CalculateWasteStress and CalculateWasteFlow .....	41

### List of Tables

<b>Table 4-1.</b> Nomenclature for Wellbore Equations.....	15
<b>Table 4-2.</b> Nomenclature for Wellbore-Repository Coupling Equations.....	19
<b>Table 4-3.</b> Nomenclature for Repository Equations.....	22
<b>Table 6-1.</b> Summary of DRSPALL Input and Output Files.....	44
<b>Table 7-1.</b> Input Parameters and Ranges .....	52
<b>Table 8-1.</b> Nomenclature for Section 8 - Test Case Control Logic .....	55
<b>Table 8-2.</b> Special variables defined for Porous Flow Test Problem .....	57

## 1 INTRODUCTION

The purpose of this document is to describe the design elements of the code DRSPALL, Version 1.00. This version of DRSPALL runs on the Alpha OpenVMS platform.

### 1.1 Software Identifier

DRSPALL, Version 1.00

### 1.2 Points of Contact

Code Sponsor: David L. Lord  
Performance Assessment & Decision Analysis Dept.  
Sandia National Laboratories  
Voice: (505)234-0055  
Fax: (505)234-0061  
e-mail: dllord@sandia.gov

Code Consultants: John Schatz  
John F. Schatz Research & Consulting, Inc.  
Del Mar, CA 92014  
Voice: (858)792-7410  
Fax: (866)848-7496  
e-mail: jschatz@jfsrc.com

David K. Rudeen  
GRAM, Inc.  
Albuquerque, NM 87112  
Voice: (505)998-0046  
Fax: (505)296-3289  
e-mail: dkrudee@sandia.gov

### 1.3 Description

DRSPALL (from Direct Release Spall) is written to calculate the volume of WIPP solid waste subject to material failure and transport to the surface as a result of an inadvertent drilling intrusion. The code calculates coupled repository and wellbore transient mixed-phase compressible fluid flow before, during, and after the drilling intrusion process. Mathematical models are included of bit penetration, mixed-phase (mud, salt, waste, and gas) fluid flow in the well, fluid expulsion at the surface, coupling of the well and the

drilled repository, repository spalling (tensile) failure, fluidized bed transport of failed waste, and repository internal gas flow. The wellbore model is one-dimensional with linear flow, while the repository model is one-dimensional with either spherical or cylindrical radial flow.

Previous work (Hansen et al., 1997) has shown that the parameter extremes most likely to be of importance to spalling releases are high repository gas pressure, low waste mechanical strength, small waste particle size (after failure), and low waste permeability. DRSPALL includes these parameters as input variables. Since conventional drilling practices are assumed in EPA regulation of the WIPP, allowance will be made for the continuous pumping of mud during drilling, the possible stoppage of the mud pump, continuous drilling after repository penetration, and the possible stoppage of drilling, based on observations made at the surface by the driller. Of course, one possibility is the continuance of pumping and drilling despite the intrusion into a high-pressure subsurface region.

Verification and validation of the main components of the DRSPALL model will be possible by comparison with other codes or independent solutions. However, it will be difficult to validate the full DRSPALL model in its entirety. Some validation can be achieved by comparison with selected analog models and experiments that have been developed by others, generally for use in the oil and gas industry. Parts of the ranges of behavior covered by these analogs should be applicable to waste repository conditions. Preparation for such work is included as part of the design process.

## 2 MAJOR CODE COMPONENTS

The major code components consist of an input control file, an optional input CDB file, the main computational loop, and output files, as shown in the following flow chart.

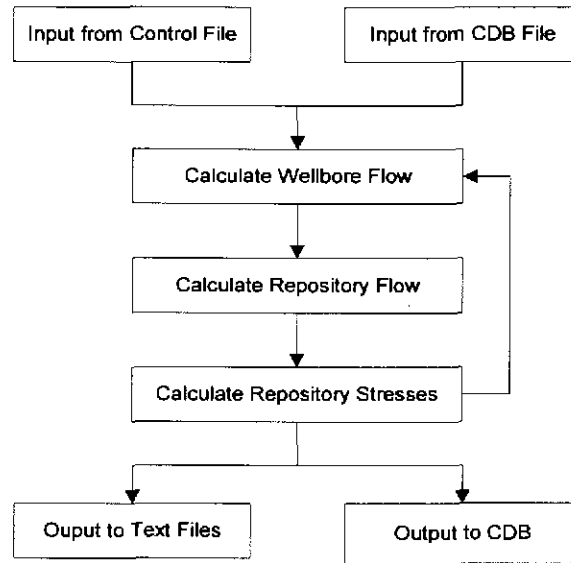


*Figure 2-1. Flow chart of major code components.*

The use of CDB files for input and output is optional. Input parameters can be provided in the input control file or read from the input CDB. However, input parameters are always echoed to the diagnostic output file. For any run, all files have the same prefix name assigned by the user, while the suffix names denote the type of file.

DRSPALL makes use of the WIPP PA libraries CAMCON\_LIB, CAMSUPES\_LIB and CAMDAT\_LIB to standardize common user interface and I/O functions and to simplify CDB access (WIPP PA 1996a, WIPP PA 1996b, WIPP PA 1996c). These libraries are linked to the DRSPALL executable during the build process as documented in the *DRSPALL Implementation Document*.

The CAMCON\_LIB library provides a library of standardized QA and user interface routines such as a code banner with credits (authors), software ID, revision date, and current date and time; file processing routines to read and parse the command line, and to specify and open files; free-field input routines; and string processing routines.

The CAMSUPES\_LIB library is a collection of machine dependent routines to access the system clock and allocate memory. However, CAMSUPES dynamic memory allocation has not been implemented in this version of DRSPALL except in the CAMDAT\_LIB library. FORTRAN 90 dynamic memory allocation is used instead.

The CAMDAT\_LIB library provides a programmer's interface through subroutine calls for accessing and creating CDB files.

### 3 THEORETICAL BASIS

DRSPALL is based on the theory of one-dimensional time-dependent compressible isothermal fluid flow. Somewhat different forms of that theory are used, depending on whether the flow is in the wellbore or in the repository, and whether the wellbore currently penetrates the repository or not. The wellbore and repository flows are coupled at a specified boundary by a set of conditions. Schematic diagrams of the flow geometry prior to and after penetration are shown in **Figure 3-1** and **Figure 3-2**, respectively. Throughout the process, the drillbit can move downward as a function of time, removing salt or waste material. Flow in the well is treated as a compressible, viscous, multi-phase mixture of mud, gas, salt, and possibly waste solids. Flow in the repository is treated as viscous, compressible single-phase gas flow in a porous solid. At the cavity forming the repository-wellbore boundary (following penetration) waste solids freed by drilling, tensile failure, and associated fluidization may enter the wellbore flow stream. Between the well and the repository, flow is treated according to the state of penetration, as described later.

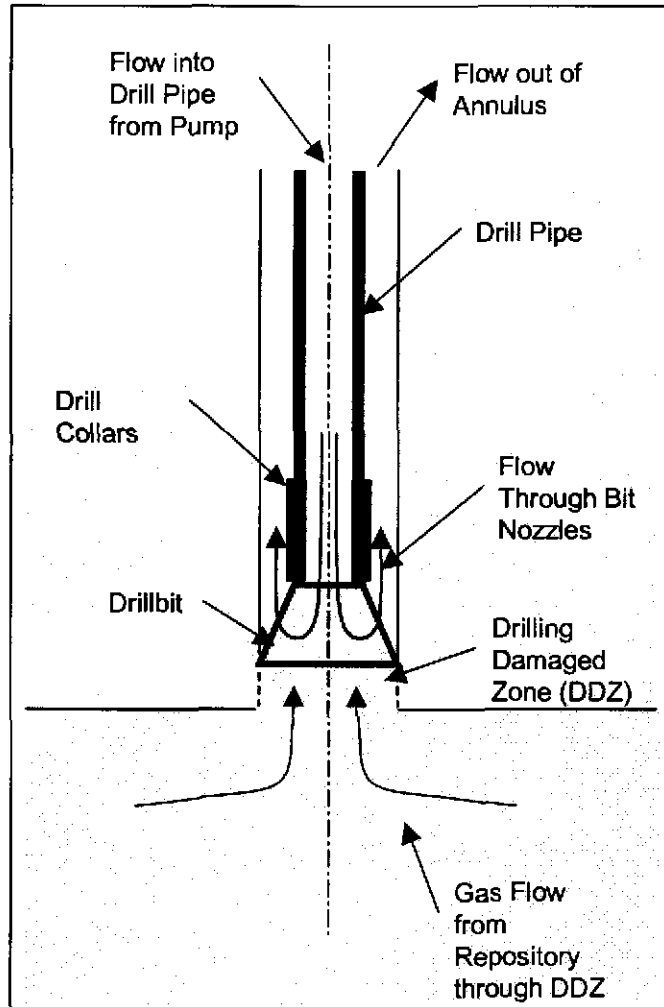


*Figure 3-1. Schematic diagram of the flow geometry prior to repository penetration.*

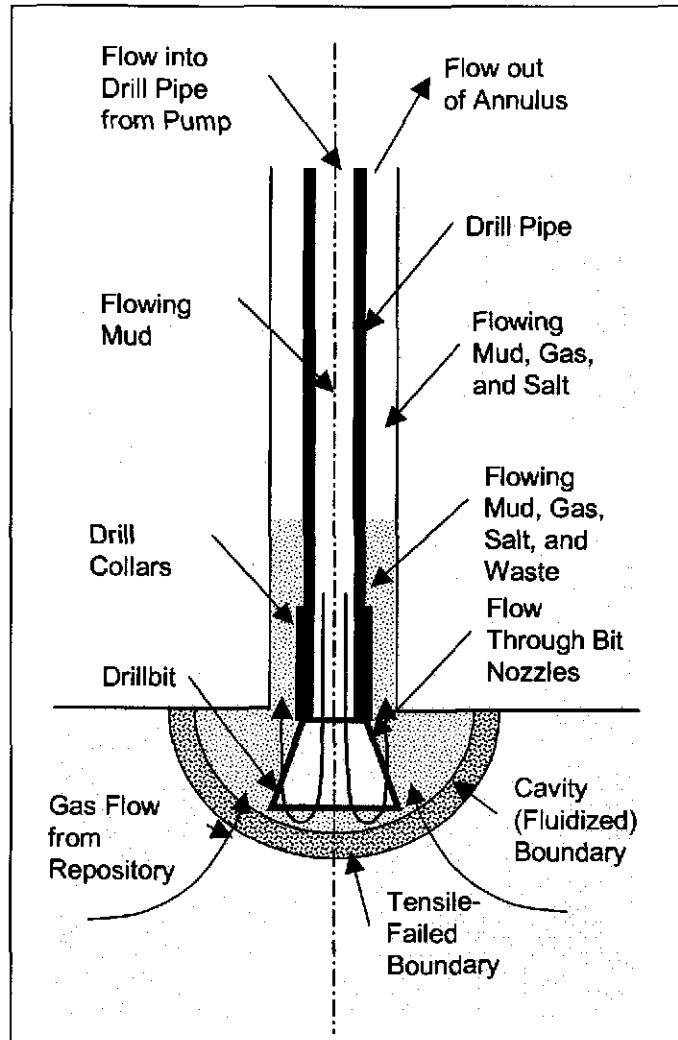


*Figure 3-2. Schematic diagram of the flow geometry after repository penetration. Spherical case is shown.*

### 3.1 Wellbore Flow Prior to Penetration

Flow in the well prior to drillbit penetration into the repository is treated as shown in Figure 3-3.

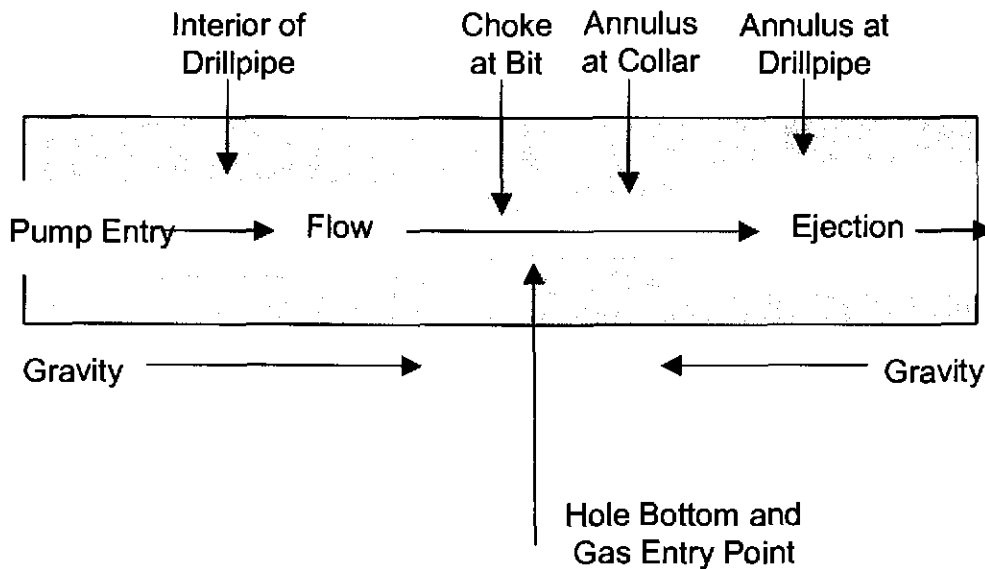


*Figure 3-3. Effective wellbore flow geometry before bit penetration.*

In concept this model is similar to that proposed by Podio and Yang, 1986, and now in use in the oil and gas industry. The pump input is controlled by volume flow rate (with a maximum pressure), and may be stopped or started. Flow is one dimensional pipe flow with cross sectional areas corresponding to the appropriate flow area at a given position in the well. The drillbit is treated as a choke with cross-sectional area appropriate to the bit nozzle area. Immediately below the bit, gas from the repository can flow through drilling-damaged salt into the well, as described in Section 3.3. After the bit, return flow to the surface is treated as pipe flow in the annulus separating the drill string and the outer hole boundary. At the annulus output to the surface, mud ejection is to a constant atmospheric pressure. The gravitational body force acts in its appropriate direction based on position before or after the bit. The well fluid is Newtonian. Viscosity of the phase mixture is determined by an approximation as discussed in Section 4.1. Flow friction may be either laminar or turbulent, also based on an approximation given in Section 4.1.

### 3.2 Repository Flow Prior to Penetration

The flow in the repository is one-dimensional radial, either hemispherical or cylindrical with its origin at the centerline of the well. Darcy flow of an isothermal ideal gas in a porous medium allows the simplifying pseudopressure approach to be taken, as is

commonly done in the field of petroleum reservoir engineering. A modification allowing for non-Darcy inertial effects at high flow velocities is included. Near the well, the boundary pressure is determined as discussed in the next section on coupling. The outer boundary of the repository is set to a no flow condition, consistent with repository far-field conditions.

Solid stresses in the repository are treated as elastic and with an effective stress law. Flow-related forces are included. A homogeneous solid is assumed. Solid stresses are not relevant prior to penetration, but play a key role in determining failure and fluidization after penetration, as discussed later.

### 3.3 Coupling of Wellbore and Repository Flow Prior to Penetration

Prior to penetration, it is assumed that the drilling action creates a cylinder of altered-permeability salt material with diameter equal to the drillbit that moves ahead of the drillbit. This material allows limited porous gas flow from the repository to the wellbore. This is shown simply as the 'Drilling Damaged Zone' or DDZ, in **Figure 3-1**. Additional conceptual detail is shown in **Figure 3-4**. The permeability of this altered zone is greater than that of the intact salt and the DRZ, and is based on a composite model as described in the Section 4.2.

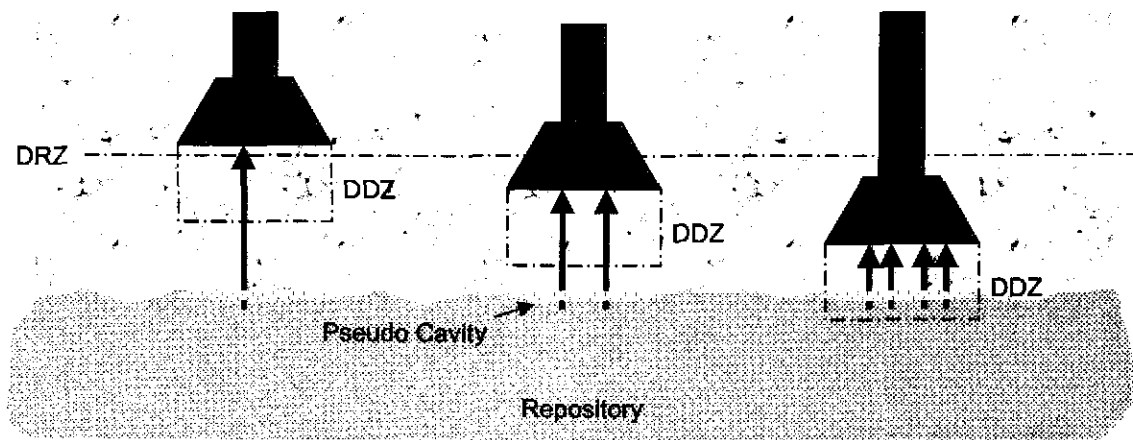


**Figure 3-4.** Coupling of the repository and wellbore prior to drillbit penetration.

Porous flow through this cylindrical volume is determined by the boundary pressures and flow areas of the volume. The boundary pressure on the well side is the pressure immediately below the bit. The area is the bit cross-sectional area (also assumed to be the wellbore area). The boundary pressure on the repository side is the pressure in a small pseudo-cavity at the wellbore face of the waste with the same surface area as the end of the drillbit. The pseudo-cavity provides continuity between the wellbore and repository and does not play a material role in total flow.

The main effect of the DDZ is to smooth the step function in pressure and flow rate that would otherwise occur upon bit penetration of the repository.

### 3.4 Wellbore Flow After Penetration

After drillbit penetration, the pseudo-cavity at the waste face becomes a real cavity and is connected to the flow area of the wellbore as shown in **Figure 3-5**. The cavity is now representative of the material removed from the repository by drilling, material failure, and subsequent fluidization.

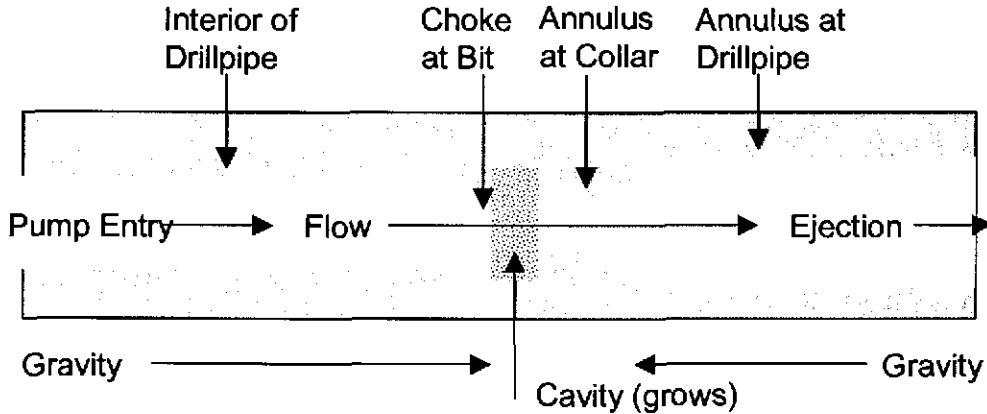


**Figure 3-5.** Effective wellbore flow geometry after bit penetration

After penetration, the cavity is treated as a mixing volume connecting the wellbore and the repository, and is used to provide the pressure boundary conditions at the inner wall of the repository. The volume of the cavity zone shown in **Figure 3-5** is constantly adjusted so that it is equal to the growing volume of the actual hemispherical or cylindrical cavity. Fluidized waste solids mix with the mud/gas/salt flow and are moved up the wellbore and possibly out at the surface. An approximate model for the viscosity of the multi-phase mixture is used. All phases in the wellbore are assumed to move at the same velocity. The assumption of a single phase velocity greatly simplifies the mathematics and speeds numerical execution time. This assumption should be conservative with respect to waste release to the surface because a lagging waste particle velocity is expected in the wellbore, leading to a lower surface release rate and lower total release. The viscosity model causes the mixed fluid to act as a dense slurry for high solids concentrations, and there is a relative solids volume which causes complete choking. Treating the fluidized cavity as a region in one-dimensional series with the wellbore flow is a simplification. However, it is consistent with the one-dimensional nature of the flows in both wellbore and repository, and is a simple and convenient way of introducing the boundary coupling without introducing more complexity than knowledge of parameters justifies.

### **3.5 Repository Flow After Penetration**

The flow model is basically the same after penetration as before. Without failure, the inner surface area of the repository is maintained at the same as the surface area of the true drilled borehole cavity. If radial tensile failure occurs as a result of pressure relief at the inner boundary and flow-related forces, the waste material is deemed susceptible to fluidization in the region of tensile failure. Then the pore fluid flow velocity is compared to a limiting velocity based on fluidized bed theory. If this fluidization velocity is exceeded, material is assumed to disaggregate and move into the cavity, thus enlarging the cavity and adding waste solids to it. The cavity volume is determined by cavity radius. The cavity radius is the sum of two components: the drilling radius and the spallings depth. The drilling radius is the radius of the volume with surface area equivalent to the surface area of the cylinder removed by drilling, as explained in section 4.4.1. The spallings depth is the depth to which fluidization extends beyond the current cavity radius, as explained in section 4.3.3.

### **3.6 Coupling of Wellbore and Repository After Penetration**

As mentioned above, the coupling of the wellbore and the repository following penetration is achieved by treating the cavity as a mixing volume. (Figure 3-5). If no fluidization occurs but drilling continues, the cavity grows at a rate equivalent to the volume being drilled. If fluidization occurs, the cavity volume may be greater than the drilled volume. Waste moves into the cavity when it is fluidized. Mass balance is maintained at all times. Mud flows into the cavity through the nozzles at the bit. Gas, waste and salt are moved into the cavity as drilling and fluidization occur. Subsequently, all components progress up the well. Salt and waste solids are treated as incompressible. Volumes of the compressible phases (gas and mud) are calculated based on their equations of state and the current pressure.

### **3.7 Preparation for Verification and Validation Testing**

Isolation of model components for testing requires special code logic for each test case. To facilitate testing using the production executable without modifications, the special logic is incorporated prior to the production build and is activated via user-controllable input switches. Warning messages are generated that clearly indicate that DRSPALL is being executed in the testing mode.

## 4 MATHEMATICAL MODEL

DRSPALL is implemented as a coupled system of differential equations and evaluated by time-marching integration. This section describes the system of equations used and the numerical techniques involved.

### 4.1 Wellbore Equations

Nomenclature is given in **Table 4-1**.

*Table 4-1. Nomenclature for Wellbore Equations.*

Symbol	Definition	Units
$A$	Flow area	$m^2$
$A_p$	Inlet area of mud pump	$m^2$
$A_{out}$	Outlet area of well	$m^2$
$c_m$	Compressibility of mud	$Pa^{-1}$
$d_h$	Hydraulic diameter	m
$D_i, D_o$	Inner and outer diameters	m
$g$	Acceleration of gravity	$m/s^2$
$i$	Zone index	--
$m_w, m_s$	Mass of waste and salt	kg
$n$	Timestep index	--
$P$	Pressure	Pa
$R_{mud\ pump}$	Volumetric rate of mud pump	$m^3/s$
$Re$	Reynold's number	--
$S$	Exponent in slurry viscosity formula	--
$S_{mass}$	Mass source term	kg/s
$S_{mom}$	Momentum source term	kg m/s <sup>2</sup>
$ss_m$	Sound speed in mud	m/s
$t$	Time	s
$u$	Velocity	m/s
$u_{out}$	Fluid velocity at outlet boundary	m/s
$V$	Volume	$m^3$
$V_w, V_s, V_g, V_m$	Volumes of waste, salt, gas, and mud	$m^3$
$w$	Volume fraction of waste solids	--
$w_{max}$	Maximum allowed value of $w$	--
$z$	Distance from pump inlet	m
$\epsilon$	Roughness of wall	m
$F$	Friction loss term	kg / m <sup>2</sup> s <sup>2</sup>
$f$	Darcy-Weisbach friction factor	--
$\eta$	Viscosity	kg / m s
$\rho$	Density	kg / m <sup>3</sup>

Symbol	Definition	Units
0	Sub or superscript denoting initial value	--

Flow in the well is transient, compressible, isothermal, viscous, and multi-phase, including a mixture of mud, gas, salt, and possibly waste solids. Leakoff to the walls is ignored. All equations are adaptations of the well-known Navier-Stokes equations for compressible fluid flow. For example, see Oran and Boris (1987). The one-dimensional conservation equations that apply in this case are, for mass balance:

$$\frac{\partial}{\partial t}(\rho V) + \frac{\partial}{\partial z}(\rho V u) = S_{mass} \quad (4.1.1)$$

and for momentum balance:

$$\frac{\partial}{\partial t}(\rho V u) + \frac{\partial}{\partial z}(\rho V u^2) = -V \left( \frac{\partial P}{\partial z} - \rho g + F \right) + S_{mom} \quad (4.1.2)$$

where the value of the dissipation term in  $F$  cannot exceed the total momentum in the current flow direction. (That is, local dissipation can slow or stop the flow, but not reverse it.) To complete the system, an equation of state relating pressure and density and the friction loss term must be defined. Also, the source term and boundary conditions must be specified.

Density  $\rho$  in Eqs. 4.1.1 and 4.1.2 is the mixture density, computed as the sum of the masses of individual phase components in a representative volume, divided by that volume. The mixture equation of state must account for the four possible mass components in the well: mud, salt, gas, and waste. Because of known initial conditions, mud pumping rate, surface effluent rate, and the gas and solidsexchange rate at the cavity-wellbore interface, the convection equations result in a known mass of each component in a given total volume. Then the individual volumes occupied by each component are determined, where

$$V = V_s + V_w + V_m + V_g \quad (4.1.3)$$

The salt and waste components are treated as incompressible, so their volumes are independent of pressure and determined from their initial user-specified densities by

$$V_s = \frac{m_s}{\rho_{0(s)}}$$

and

$$V_w = \frac{m_w}{\rho_{0(w)}} \quad (4.1.4)$$

The gas is treated as isothermal and ideal, so

$$\rho_g = \rho_{0(g)} \frac{P}{P_0} \quad (4.1.5)$$

The mud is assumed to be a compressible liquid, so

$$\rho_m = \rho_{0(m)} [1 + c_m (P - P_0)] \quad (4.1.6)$$

where  $P_0$  is atmospheric pressure. To calculate pressure at a given location, note that the masses and total volume will always be known. Also, the volumes of salt and waste will be known, since they are considered incompressible. This means the total combined volume of gas and mud are known. This allows Eqs. (4.1.5) and 4.1.6) to be combined, resulting in a quadratic equation for gas volume.

$$aV_g^2 + bV_g - c = 0 \quad (4.1.7)$$

where,

$$\begin{aligned} a &= 1 - C_m P^0 \\ b &= (C_m P^0 V_g^0 - aV^* + V_m^0) \\ c &= V^* C_m P^0 V_g^0 \end{aligned}$$

and

$$V^* = V_m + V_g = V - V_s - V_w$$

Once gas volume is known, densities can be determined and pressure can be evaluated from either the gas (4.1.5) or mud equation of state (4.1.6).

For friction loss, a standard formulation for pipe flow is used (Fox and McDonald, 1985), where the head loss per unit length is given as:

$$F = f \frac{\rho u^2}{d_h 2} \quad (4.1.8)$$

The hydraulic diameter  $d_h$  is given by

$$d_h = \frac{4A}{\pi(D_i + D_o)} \quad (4.1.9)$$

Note that for flow in the drill pipe,  $D_i = 0$ . For annular flow up the wellbore,  $D_i$  is the outer diameter of the drill pipe and  $D_o$  is the wellbore diameter.

#### 4.1.1 Wellbore friction factor

The friction factor  $f$  is determined by the method of Colebrook (Fox and MacDonald, 1985). In the laminar regime ( $Re < 2100$ )

$$f = \frac{64}{Re} \quad \text{where} \quad Re = \frac{u \rho d_h}{\eta} \quad (4.1.10)$$

In the turbulent regime ( $Re > 2100$ )

$$\frac{1}{\sqrt{f}} = 2.0 \log \left( \frac{\varepsilon/d_h}{3.7} + \frac{2.51}{Re\sqrt{f}} \right) \quad (4.1.11)$$

An approximate solution for Colebrook's  $f$  in the turbulent regime is given by Serghides (1984):

$$a = -2 \log \left[ \frac{\varepsilon/d_h}{3.7} + \frac{12}{Re} \right] \quad (4.1.12)$$

$$b = -2 \log \left[ \frac{\varepsilon/d_h}{3.7} + \frac{2.51a}{Re} \right] \quad (4.1.13)$$

$$c = -2 \log \left[ \frac{\varepsilon/d_h}{3.7} + \frac{2.51b}{Re} \right] \quad (4.1.14)$$

$$f = \left[ a - \frac{(b-a)^2}{c+a-2b} \right]^{-2} \quad (4.1.15)$$

#### 4.1.2 Viscosity of wellbore slurry

As the wellbore mixture becomes particle-laden, the viscosity of the mixture is determined from an empirical relationship developed for proppant slurry flows in channels for the oil and gas industry (Barree and Conway, 1995). First, a base fluid viscosity  $\eta_0$  is determined by relative volume-weighting of the user-specified viscosities of the mud and gas. Then this viscosity is modified by an approximate slurry formula based on the volume fraction of waste solids.

$$\eta = \eta_0 \left( 1 - \frac{w}{w_{max}} \right)^s \quad (4.1.16)$$

An important assumption is that the particle diameter of the solids is always less than the

channel width. If  $w$  reaches or exceeds its maximum value  $w_{max}$ , effective viscosity becomes large, and the flow chokes. Both  $w_{max}$  and  $s$  are empirically determined.

### 4.1.3 Wellbore boundary conditions

At the pump inlet, the source terms  $S_{mass}$  and  $S_{mom}$  are set by the volume flow rate of the pump and the density of the mud at the inlet such that

$$S_{mass} = \rho_{0(m)} R_{mudpump} \quad (4.1.17)$$

and

$$S_{mom} = \frac{\rho_{0(m)}}{A_p} R_{mudpump}^2 \quad (4.1.18)$$

The outlet boundary at the surface uses a specified pressure, usually set to atmospheric pressure. This contributes to setting  $dP/dz$  at the outlet boundary in Eq. (4.1.2) and the resulting outlet boundary velocity sets the outlet source terms as

$$S_{mass} = -\rho A_{out} u_{out} \quad (4.1.19)$$

and

$$S_{mom} = -\rho A_{out} u_{out}^2 \quad (4.1.20)$$

Additionally, mass input sources, as specified in sections 4.2 and 4.4, occur at a point corresponding to the porous flow across the drilling damaged zone prior to penetration and at a point corresponding to the cavity wall after penetration. No momentum is assumed to be contributed by these inputs.

## 4.2 Wellbore-Repository Coupling Equations Prior to Penetration

Nomenclature is given in Table 4-2.

**Table 4-2. Nomenclature for Wellbore-Repository Coupling Equations.**

Symbol	Definition	Units
$A_{cav}$	Outer area of pseudo cavity	$m^2$
$d_{bit}$	Diameter of drillbit	m
$H_o$	Thickness of repository prior to closure	m
$H$	Current thickness of repository	m
$k_{eff}$	Effective permeability of cylinder	$m^2$
$k_{DDZ}$	Permeability of DDZ	$m^2$
$k_{DRZ}$	Permeability of DRZ	$m^2$
$L$	Total length of cylinder	m

Symbol	Definition	Units
$L_{DDZ}$	Length of cylinder in DDZ	m
$L_{DRZ}$	Length of cylinder in DRZ	m
$m_{cav}$	Mass of gas in pseudo cavity	kg
$m_{cyl}$	Mass of gas flowing from cylinder	kg
$P_{cav}$	Pressure in repository pseudo cavity	Pa
$P_{BH}$	Pressure in bore hole just ahead of bit	Pa
$T$	Temperature	K
$R_0$	Ideal gas constant	J/kg·K
$\eta$	Gas viscosity	kg/m s
$\phi_0$	Porosity of a waste-filled room prior to closure	--
$\phi$	Current repository porosity	--
$\rho_g$	Density of gas	kg/m <sup>3</sup>

Prior to penetration, the cylinder of altered permeable salt connecting the wellbore and the repository has a permeability and gas flow rate determined by the series connection of the salt, DRZ, and DDZ permeability (Gross and Thompson, 1998). Since the DDZ permeability is the greatest of these, and the DRZ boundary is fixed while the DDZ boundary advances with drilling, and  $L$  is decreasing with time, the permeability of this zone decreases with time and becomes unbounded as the repository is penetrated. However, since the cavity and borehole pressures converge as the repository is penetrated, the overall mass flow remains bounded. If we start the process at the moment the DRZ or DDZ is contacted (whichever is most above the repository) the mass flow rate thus defined is determined by an incrementally steady-state solution to Darcy's equation for compressible flow (Gross and Thompson, 1998)

$$\frac{dm_{cyl}}{dt} = \frac{k_{eff} \pi \left( \frac{d_{bit}}{2} \right)^2}{2\eta R_0 TL} (P_{cav}^2 - P_{BH}^2) \quad (4.2.1)$$

where

$$k_{eff} = \frac{L}{\frac{L_{DDZ}}{k_{DDZ}} + \frac{L_{DRZ}}{k_{DRZ}}} \quad (4.2.2)$$

There is no need to start this process while there is intact salt between the DDZ and repository, as the flow is too small to have noticeable effect. In the numerical analysis, a series of steady-states (one for each timestep) is used with time-varying pressure boundary conditions. The wellbore pressure boundary is the pressure at the point of entry (just below the bit) and the repository pressure is that of the small pseudo cavity at the face of the repository. Although the flow is not truly steady-state, this approach is justified as follows: When the distance  $L$  is large (that is, drilling is at or above the DRZ) the steady state assumption will somewhat overestimate the flow, but the flow itself is so

small that the error is small. When the distance  $L$  becomes small, the steady-state assumption becomes more and more accurate, since equilibrium is rapidly achieved. Thus the stepwise steady state approach becomes sufficiently accurate at the time and position of the bit where accuracy is most required. These conclusions are established by inspection of the results of (Gross and Thompson, 1998).

Repository thickness  $H$  at the time of intrusion is determined from the current repository porosity  $\phi$ , and the height  $H_o$  and porosity  $\phi_o$  of a waste-filled room prior to closure:

$$H = \frac{(1 - \phi_o)H_o}{1 - \phi} \quad (4.2.3)$$

To couple to the wellbore, Eq. (4.2.1) is used as the source term,  $S_{mass}$ , in Eq. (4.1.1) for the wellbore, at the leading edge of the bit. To couple to the repository, the pseudo cavity is created below the bit centered at the point where penetration will eventually occur. The geometry of the pseudo cavity is a hemisphere with outer area equal to the bit area in the spherical case, or a cylinder with outer area equal to the bit area in the cylindrical case. The volume of this cavity is thus, for example, in the spherical case

$$V_{cav} = \left( \frac{\pi}{24\sqrt{2}} \right) d_{bit}^3 \quad (4.2.4)$$

and in the cylindrical case

$$V_{cav} = \left( \frac{\pi}{64H} \right) d_{bit}^4 \quad (4.2.5)$$

If the pseudo cavity volume is small compared to physical volumes in the system, it will act to provide compatible boundary conditions prior to penetration and should have no other effect on the solution. For example, once the bit has penetrated the repository by about 1/10 its diameter, the volume actually drilled in the repository exceeds that volume of the pseudo cavity. The pseudo cavity starts at repository pressure and contains gas. Mass flow out of the pseudo cavity is defined by Eq. (4.2.1). Mass flow into the cavity is defined by the pressure gradient at the repository cavity wall and other permeable flow parameters

$$\frac{dm_{cav}}{dt} = \rho_{g(repos)} u_{repos} \phi A_{cav} \quad (4.2.6)$$

where the density and velocity are defined in the repository at the cavity wall boundary. Once the net mass flow into/out of the cavity is determined, the pressure in the cavity is determined from the ideal gas law.

### 4.3 Repository Equations

Nomenclature is given in Table 4-3.

*Table 4-3. Nomenclature for Repository Equations.*

Symbol	Definition	Units
$a$	Particle shape factor	--
$C_0$	Cohesion	Pa
$d_p$	Diameter of particles (mean)	m
$F_f$	Fraction of material fluidized	--
$F_0$	Forchheimer number	--
$g$	Acceleration of gravity	m/s <sup>2</sup>
$i, j$	Zone indices	--
$k,$	Permeability	m <sup>2</sup>
$k'$	Velocity dependent permeability	m <sup>2</sup>
$k_f$	Permeability in failed material	m <sup>2</sup>
$L_t$	Characteristic length for tensile failure	m
$m$	Geometry exponent (m=3 for spherical, m=2 for cylindrical)	--
$p$	Pressure in gas	Pa
$p_c$	Pressure at cavity face	Pa
$p_{ff}$	Pressure in far-field	Pa
$p_m'$	Mean normal effective stress	Pa
$r$	Radius	m
$r_{cl}$	Radius at center of first intact cell	m
$r_c, r_{equiv}$	Radius at cavity face	m
$S_0$	Shear strength	Pa
$t$	Time	s
$t_f$	Fluidization time	s
$t_m$	Mixing time from store to cavity	s
$T_0$	Tensile strength	Pa
$U_f$	Fluidization velocity	m/s
$U_s$	Superficial gas velocity	m/s
$\beta$	Biot's constant (near 1.0)	--
$\beta_{nd}$	Non-Darcy coefficient	1/m
$\Delta H$	Current bit penetration	m
$\eta$	Viscosity of gas	kg/m s
$\psi$	Pseudopressure	Pa m <sup>2</sup> /s
$\rho$	Density of gas	kg/m <sup>3</sup>
$\rho_w$	Density of waste solids	kg/m <sup>3</sup>
$\sigma_{ff}$	Stress in far-field	Pa
$\sigma_{sr}, \sigma_{s\theta}$	Radial and tangential seepage stresses	Pa

Symbol	Definition	Units
$\sigma_r', \sigma_\theta'$	Radial and tangential effective stresses	Pa
$\tau$	Maximum shear stress	Pa
$\theta$	Angle of internal friction	rad., deg.
$\mu$	Friction coefficient	--
$\nu$	Poisson's ratio	--
$\zeta_m, \zeta_p$	Numerical diffusion coefficient for mass and momentum, respectively	--

Flow in the repository is transient, compressible, viscous, and single phase for a porous diffusive solid. The one-dimensional equations that apply in this case are as follows (Chan et al., 1993).

$$\frac{\partial p}{\partial t} = \frac{k'}{2\phi\eta} \nabla^2(p^2) \quad (4.3.1)$$

where the operator is given by

$$\nabla^2 = \frac{1}{r^{m-1}} \frac{\partial}{\partial r} \left( r^{m-1} \frac{\partial}{\partial r} \right) \quad (4.3.2)$$

For an isothermal ideal gas, the pseudopressure is

$$\psi = \frac{p^2}{\eta} \quad \text{or} \quad p = \sqrt{\eta\psi} \quad (4.3.3)$$

Combining Eqs. (4.3.1), (4.3.2), and (4.3.3) leads to

$$\frac{\partial \psi}{\partial t} = \frac{D(\psi)}{r^{m-1}} \frac{\partial}{\partial r} \left( r^{m-1} \frac{\partial \psi}{\partial r} \right) \quad (4.3.4)$$

$$\text{where } D(\psi) = \frac{k'}{\phi} \sqrt{\frac{\psi}{\eta}} = \frac{k'p}{\phi\eta}$$

Since the equation of state is embedded in the pseudopressure definition as used here, no additional equation relating gas pressure and density is needed.

The singularity as  $r$  approaches zero in Eq. (4.3.4) is not a concern since the cavity/repository boundary always occurs at finite  $r$  and the repository equation never has to be solved for  $r$  approaching zero. The boundary conditions at the inner radius of the repository are discussed in Sections 4.2 and 4.4. The condition at the outer boundary is based on no flow with an initial pressure equal to the repository pressure.

#### 4.3.1 Non-Darcy Flow

The gas flow rates near the cavity boundary may be quite high and cause an inertial resistance to flow (Belhaj et al., 2003). (Some early authors used turbulence as an explanation for the effect but most recent authors confirm that the flow is laminar, but

tortuous.(Hassanizadeh and Gray, 1987).) To account for the effect, we use a modification to the Darcy flow equation commonly called the Forchheimer effect, which we express as a velocity-dependent permeability reduction. A second term in velocity squared is added to the Darcy equation.

$$-\frac{\partial P}{\partial x} = \frac{\eta}{k}u + \beta_{nd}\rho u^2 \quad (4.3.5)$$

This equation can be expressed in the form

$$-\frac{\partial P}{\partial x} = \frac{\eta}{k'}u \quad (4.3.6)$$

where

$$k' = \frac{k}{1 + F_0} \quad \text{and} \quad F_0 = \frac{\beta_{nd}\rho k u}{\eta} \quad (4.3.7)$$

The Forchheimer number  $F_0$  has sometimes been called the Reynold's number for porous flow. The non-Darcy coefficient  $\beta_{nd}$ , which depends on material properties such as the tortuosity and area of internal flow channels, is empirically determined. We choose a study by Li et al., 2001 which used high-velocity nitrogen flow through porous sandstone wafers, giving the result ✓

$$\beta_{nd} = \frac{1.15 \times 10^{-6}}{k\phi} \quad (4.3.8)$$

Other published values and mathematical forms exist and can vary when evaluated by as much as an order of magnitude from Eq. (4.3.8). This form was chosen for mathematical simplicity, because it represents neither the high nor the low end of the range, and because it is one of the studies that specifically looked at gas flow in highly porous materials with a large number of measurements. Within DRSPALL, an exact solution including the Forchheimer effect would require expressing Eq. (4.3.5) in radial coordinates and solving the new repository flow equation. The simplifying pseudopressure approach would no longer apply. Instead, the approach described here, of a simple modification to permeability is chosen. Not only is this much more convenient mathematically, but it is entirely consistent with the expected range of accuracy of solutions, given the variation in empirical results.

The impact of including the velocity squared term in the Darcy equation on the flow equation (4.3.1) can be evaluated by re-deriving the flow equation using (4.3.5), (4.3.7), the equation of state:

$$P = P_0 \frac{\rho}{\rho_0} \quad (4.3.9)$$

and the conservation of mass:

$$\varphi \frac{\partial \rho}{\partial t} + \frac{\partial}{\partial x}(\rho u) = 0 \quad (4.3.10)$$

which gives:

$$\frac{\partial P}{\partial t} = \frac{k'}{2\varphi\eta} \nabla^2 P^2 + \frac{1}{2\varphi\eta} (P\nabla P) \nabla(k') \quad (4.3.11)$$

DRSPALL assumes the second term on the right hand side is small relative to the first which results in flow equation (4.3.1) in terms of the velocity dependent permeability  $k'$ :

$$\frac{\partial P}{\partial t} = \frac{k'}{2\varphi\eta} \nabla^2 P^2 \quad (4.3.12)$$

### 4.3.2 Elastic Response and Failure

To determine failure and fluidization, solid elastic effective stresses are required. While the fluid calculations using Eq. (4.3.4) are fully transient, the solid stress calculations are assumed to be quasi-static. (That is, we ignore sound-speed phenomena in the solid.) The stress equations are thus found as follows.

Elastic effective stresses are (Jaeger and Cook, 1969):

$$\sigma_r'(r) = \sigma_{sr}(r) + \sigma_{ff} \left[ 1 - \left( \frac{r_c}{r} \right)^m \right] + p_c \left( \frac{r_c}{r} \right)^m - \beta p(r) \quad (4.3.13)$$

$$\sigma_{\theta}'(r) = \sigma_{s\theta}(r) + \sigma_{ff} \left[ 1 + \frac{1}{(m-1)} \left( \frac{r_c}{r} \right)^m \right] - \frac{p_c}{(m-1)} \left( \frac{r_c}{r} \right)^m - \beta p(r) \quad (4.3.14)$$

where the flow-related stresses are given by (in analogy to differential thermal expansion, Timoshenko and Goodier, 1970):

$$\sigma_{sr}(r) = (m-1)\beta \left( \frac{1-2\nu}{1-\nu} \right) \frac{1}{r^m} \int_{r_c}^r [p(r) - p_{ff}] r^{m-1} dr \quad (4.3.15)$$

$$\sigma_{s\theta}(r) = -\beta \left( \frac{1-2\nu}{1-\nu} \right) \left( \frac{1}{r^m} \int_{r_c}^r [p(r) - p_{ff}] r^{m-1} dr - [p(r) - p_{ff}] \right) \quad (4.3.16)$$

Since stresses are calculated as quasi-static, an initial stress reduction caused by an instantaneous pressure drop at the cavity face propagates instantaneously through the waste. The result of calculating Eq. (4.3.14) can be an instantaneous early-time tensile failure of the entire repository if the boundary pressure is allowed to change suddenly. This is non-physical and merely a result of the quasi-static stress assumption combined with the true transient pore pressure and flow-related stress equations. To prevent this behavior, tensile failure is not allowed until the propagation distance determined by a tensile propagation limit ("tensile failure velocity", Hansen et al., 1997), beginning at the cavity face, occurs. This should have no quantitative effect on results other than to

prevent a non-physical tensile failure occurring at initial wellbore penetration. It is possible that allowing pre-penetration flow through the DDZ as described in Section 4.2 renders the introduction of this procedure unnecessary.

For tensile failure, the radial effective stress is averaged from the cavity boundary into the waste over a characteristic length  $L_r$ . If this average stress is tensile and exceeds the material tensile strength,  $T_0$ , the waste is assumed to be no longer capable of supporting radial stress, and the material from the cavity out to the characteristic length  $L_r$  is marked as failed. After failure, fluidization is allowed in the failed material. The cavity boundary does not move outward until after the failed material fluidizes, as discussed in sections 4.3.3 and 4.3.5.

Potential shear failure locations are determined (flagged), but no relaxation associated with shear failure is used. For shear failure, the maximum shear stress

$$\tau(r) = \frac{1}{2} |(\sigma_r'(r) - \sigma_\theta'(r))| \quad (4.3.17)$$

and mean normal effective stress

$$p_m'(r) = \frac{[\sigma_r'(r) + (m-1)\sigma_\theta'(r)]}{m} \quad (4.3.18)$$

are used to determine if maximum shear stress exceeds the linear Mohr-Coulomb shear strength

$$\tau(r) > S_0 + \mu p_m'(r) \quad (4.3.19)$$

where

$$S_0 = \frac{C_0}{2} \left[ \mu + (\mu^2 + 1)^{\frac{1}{2}} \right] \quad (4.3.20)$$

and

$$\mu = \tan(\theta) \quad (4.3.21)$$

Again, singularities as  $r$  approaches zero are avoided because of the always-finite cavity. The solid stress boundary conditions are, for the inner boundary, no shear stress and radial stress equal to cavity pressure. For the outer boundary, the far field confining (radial) stress is set as an input parameter. There is no far-field shear stress.

### 4.3.3 Fluidization

In a region where tensile failure has occurred, the waste material is first assumed to be disaggregated, but not in motion. It remains as porous, bedded material lining the cavity face, and is treated as a continuous part of the repository from the perspective of the porous flow calculations. The bedded material is subject to mobilization and removal to the flow stream in the cavity by fluidized bed theory. As such, solids are allowed to flow into the cavity if the superficial gas velocity,  $U_s$ , at the cavity face exceeds a minimum fluidization velocity,  $U_f$ . Superficial gas velocity is defined as the average velocity across

the entire surface area of the cavity ( $U_s = \text{pore velocity} \times \phi$ ). The cavity radius will increase corresponding to the volume of solid material removed by fluidization. The minimum fluidization velocity is determined by solving the following quadratic equation (Cherimisinoff and Cherimisinoff, 1984; Ergun, 1952).

$$\frac{1.75 \left( \frac{d_p U_f \rho}{\eta} \right)^2}{a \phi^3} + 150 \left( \frac{1 - \phi}{a^2 \phi^3} \right) \left( \frac{d_p U_f \rho}{\eta} \right) = \frac{d_p^3 \rho (\rho_w - \rho) g}{\eta^2} \quad (4.3.22)$$

If fluidization occurs, the cavity is allowed to grow until the cavity radius equals the depth of the first intact (non tensile-failed) material. New tensile failure is allowed from the boundary into the intact repository material. Once the entire region of length  $L_i$  nearest boundary fluidizes, a new region of length  $L_i$  is defined and evaluated for failure as discussed above. With cavity growth, the gas and waste particles in the newly fluidized region must mix into the cavity in such a way as to conserve mass. To account for the fact that this mixing cannot be instantaneous, which would be non-physical and lead to numerical instability later (much as allowing instantaneous tensile failure propagation), a small artificial relaxation time, equal to the cavity radius divided by the superficial gas velocity, is imposed upon the mixing phenomenon. As fluidization occurs, the permeability of the failed waste in that region is allowed to grow according to

$$k_f = k'(1 + 4F_f) \quad (4.3.23)$$

Where  $F_f$  is the fraction fluidized and is based on the fluidization relaxation time. This approximately accounts for the bulking of material as it fluidizes. It is interesting to note that the Ergun equation, which leads to Eq. 4.3.22, can also be used to derive a non-Darcy coefficient for particulate beds (Narayanaswamy et al., 1999). This takes a similar form to Eq. 4.3.8 (but not the same value). This suggests, as would be expected, that there is continuous transition from intact to failed to fluidized material. However, we expect that the accuracy required by the present work does not require further investigation of this transition.

#### 4.3.4 Repository Boundary Conditions

The porous flow equations are solved with a pressure (flow) boundary condition at the inner (cavity) wall and a zero pressure gradient (no-flow) condition at the outer wall. For the inner wall, the cavity pressure (either pseudo or real) sets a pressure outside the porous solid. The inner cavity wall propagates radially outward as material is drilled or failed and fluidized and moved from the repository to the cavity. Thus, the boundary condition is subsequently applied to the adjacent non-fluidized but possibly failed material. The pressure inside the porous solid then develops a gradient, based on the pressure difference, which is used to calculate a pore velocity at the boundary using Darcy's Law:

$$u_{repos} = \frac{k}{\eta \phi} \frac{\partial p}{\partial r} \Big|_{r=r_c} \quad (4.3.24)$$

Material (gas) loss across the boundary as a function of time can then be calculated using equation (4.2.6).

#### 4.3.5 Implementation of conceptual submodels in DRSPALL

Some of the features of the conceptual and mathematical model discussed earlier require special implementation procedures in a finite difference code. The purpose of this section is to elucidate the implementation steps that are not necessarily clear in a discussion of the conceptual model alone.

##### 4.3.5.1 Characteristic length and tensile failure

A review of the effective stress formulation (Eq. 4.3.13) reveals several issues that require careful consideration when applying this model to a repository domain divided into discrete computational zones. A typical radial effective stress curve is drawn in Figure 4-1. The tensile strength of the waste is shown in the figure as well. Effective radial tensile stresses (negative values on the stress axis) are shown to develop near to, but not exactly at the cavity wall. In fact, the effective stress exactly at the cavity wall is always  $\sigma_r'(r_c) = 0$ . As such, a region of tension develops that may exceed the tensile strength at radii greater than, but not at, the cavity wall. The region of material subject to tensile failure, without consideration of the characteristic length concept, is circled in Figure 4-1. Note that material between the failed region and the cavity wall is still intact according to the current stress model.

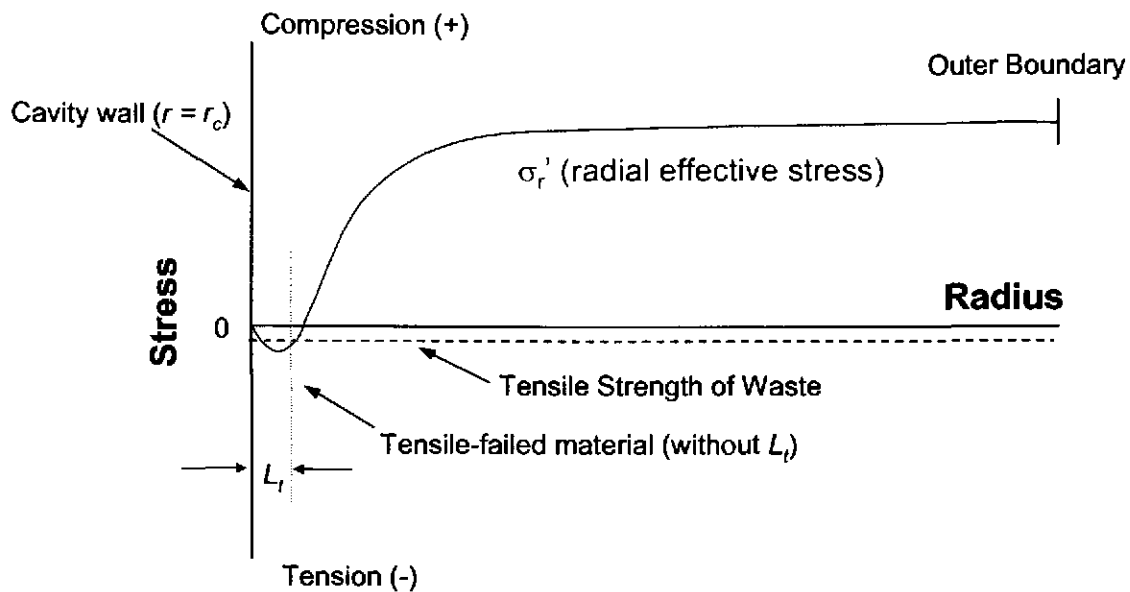


**Figure 4-1.** Drawing of typical radial effective stress curve in DRSPALL repository domain at some time during drill penetration.

Failed regions trapped between intact shells cannot, by themselves, be removed from the repository domain without first removing the intact cavity wall. It is proposed here that once a tensile-failed region exists, the cavity wall is likely to eventually succumb to buckling failure. A simple approach to this is implemented in DRSPALL by introducing a characteristic failure length  $L_t$  in which the mean tensile stress is evaluated over a region that extends from the cavity wall ( $r = r_c$ ) to a depth of one characteristic length ( $r = r_c + L_t$ ) into the domain. This characteristic length must be large enough to encompass several computational zones, but not so large that it masks the tensile region. If the mean tensile stress over  $L_t$  exceeds the tensile strength, all the zones in  $L_t$  fail, and they are flagged as “failed” in DRSPALL. Zones outside of  $L_t$  are not allowed to fail until all the disaggregated, bedded waste is fluidized.

#### 4.3.5.2 Cavity growth by drilling

During normal drilling, when the bit penetration depth passes the outer edge of a computational zone, that zone (gas and solids) is removed from the repository domain and put into “store.” From store, the drilled mass is then released to the cavity over a mixing time  $t_m = (r_{cl}/U_s)$  where  $r_{cl}$  is the center of the cell that forms the cavity wall ( $r_{cl} = r_c + 1/2\Delta r$ ). This is done because instantaneously adding the entire contents of one computational zone to the cavity causes numerical noise, and the controlled release from store dampens the numerical shock.

#### 4.3.5.3 Cavity growth by fluidization

In the event that a group of zones comprising  $L_t$  fails, the zones are all tested for fluidization potential using the Ergun (1952) model given in Eq. 4.3.22. If the superficial gas velocity exceeds the minimum fluidization velocity ( $U_s > U_f$ ), all failed zones are flagged for fluidization. The fluidization process requires a finite fluidization time  $t_f = r_{cl}/U_s$ . Zones must begin fluidization sequentially so that the zone comprising the cavity wall starts first, after which the next zone can start fluidization on the very next timestep. This proceeds until all zones flagged for fluidization are removed from the repository domain and thus incorporated into the wellbore domain. The cavity thus grows in zone-by-zone increments as subsequent zones complete fluidization.

### 4.4 Wellbore-Repository Coupling Equations Following Penetration

Upon penetration by the drillbit, the porous flow Eq. (4.2.1) at the drillbit/cavity inner boundary is no longer used. Instead, the cavity volume is assumed to be included in the wellbore flow path as shown in **Figure 3-4**. If the cavity subsequently grows due to drilling, tensile failure and fluidization, the volume of this part of the flow path increases to be consistent with the growing cavity volume. The equivalent physical assumption is that mud flow passes through the bit nozzles, mixes fully with the gas and waste in the cavity and then the resulting mixture flows up the annulus around the drill collars. Thus no new equations are needed, other than to be sure that mass balance is maintained and that cavity volume is correct. Eq. (4.2.6) is still used to determine gas mass flow into the cavity from the repository. Waste flows into the cavity by simply mixing in fluidized

waste as discussed in Section 4.3. The mass input provided by gas and waste flowing into the cavity replace the gas mass source provided by the DDZ prior to penetration, thus mathematical consistency and continuity are maintained throughout the drilling and gas/waste flow process.

#### 4.4.1 Geometry-Dependent Equivalent Drilled Radius

The true cylindrical cavity of increasing height formed during the drilling process must be mapped each computational step to an equivalent cavity radius in the specified one-dimensional spherical or cylindrical geometry. This mapping assumes conservation of surface area in order to preserve the early time repository pressure gradients and thus gas flux from the repository to the wellbore. Note that the drilled volume will not be conserved.

The surface area of the true cylinder cut from the waste takes the shape of a soup can with one end removed. The surface area of this cut cylinder is therefore:

$$A_{cut} = \frac{\pi d_b^2}{4} + \pi d_b \Delta H \quad (4.4.1)$$

In spherical geometry the equivalent radius is determined by equating  $A_{cut}$  with the surface area of a hemisphere ( $A = 2\pi r_{eq}^2$ ). Solving for  $r_{eq}$  gives:

$$r_{eq} = \left( \frac{A_{cut}}{2\pi} \right)^{\frac{1}{2}} \quad (4.4.2)$$

In cylindrical geometry the equivalent radius is determined by equating  $A_{cut}$  with the surface of a cylinder with fixed height  $H$  and open ends ( $A = \pi d_b H$ ). Solving for  $r_{eq}$  in this case gives:

$$r_{eq} = \left( \frac{A_{cut}}{2\pi H} \right) \quad (4.4.3)$$

For small penetration depths this implies a very small diameter equivalent cylinder with a height equal to the repository thickness.

Equivalent volumes are calculated from the equivalent radius using the volume equation appropriate for the assumed geometry. When the bit reaches the floor of the repository, drilling is stopped and in cylindrical geometry the actual drilled and equivalent volumes will be the same. But, in spherical geometry the equivalent volume will be greater than the drilled volume.

#### 4.5 Numerical Method – Wellbore

Both the wellbore and the repository calculations use time-marching finite differences. These are part of a single computational loop and therefore use the same time step. The differencing schemes for the wellbore and repository calculations are similar but not identical.

The wellbore is zoned for finite differencing as shown in **Figure 4-2**. This shows zones, zone indices, grid boundaries, volumes, and interface areas. The method is Eulerian. That is, zone boundaries are fixed, and fluid moves through the interfaces by convection. Quantities are zone-centered and integration is explicit in time. In the following, detailed discussion will be specific to the mass transport given by Eq. (4.1.1). However, the differencing method for the momentum transport given by Eq. (4.1.2) is the same.

The equations shown below are for constant zone size. DRSPALL actually implements difference equations that allow for the zone size to vary from cell to cell. The intent is to use small zones near regions where there are geometry changes and grow them geometrically away from those regions.

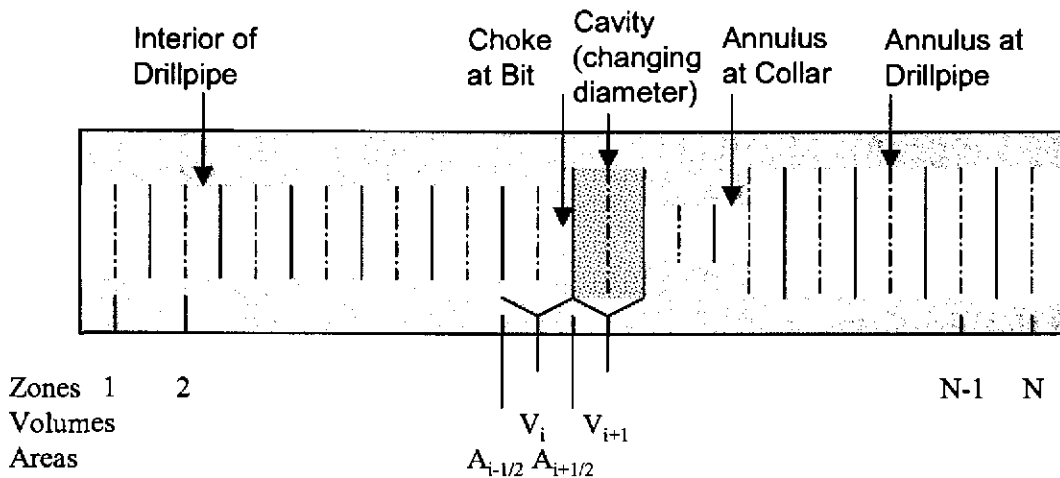


**Figure 4-2** Finite difference zoning for wellbore.

All of the materials (mud, salt, gas, and waste) are assumed to move together as a mixture. Since fluid moves through the grid boundaries, calculation requires values for the flow through these boundaries during a timestep. This is obtained from difference between the fluid velocities at the zone centers, given by

$$u_{i+1/2} = \frac{1}{2} (u_{i+1}^{n-1} + u_i^{n-1}) \quad (4.5.1)$$

The mass transport equation, prior to any volume change, becomes

$$V_i \rho_i^* = V_i \rho_i^{n-1} - \Delta t (A_{i+1/2} \rho_{i+1/2}^{n-1} u_{i+1/2} - A_{i-1/2} \rho_{i-1/2}^{n-1} u_{i-1/2}) + \Delta t S_{m,i} \quad (4.5.2)$$

Here the source terms ( $S_{m,i}$ ) are set to correspond to material entering or exiting at the pump, cavity, and surface. The “upwind” zone centered densities are used for the interfaces values,  $\rho_{i+1/2}^{n-1}$  and  $\rho_{i-1/2}^{n-1}$ .

Finally we incorporate any changed volumes and add numerical mass diffusion for stability:

$$V_i \rho_i^n = V_i \rho_i^* + \Delta z \sum_{m=1}^{N_c} \zeta_m \left[ A_{i+1/2} \left( (\rho f_m)_{i+1}^{n-1} - (\rho f_m)_i^{n-1} \right) - A_{i-1/2} \left( (\rho f_m)_i^{n-1} - (\rho f_m)_{i-1}^{n-1} \right) \right] \quad (4.5.3)$$

The densities,  $\rho f_m$ , are for the particular constituent,  $m$ , being diffused and are calculated from the mixture density,  $\rho$ , time the mass fraction,  $f_m$ , of the constituent in the referenced cell. The numerical diffusion coefficient  $\zeta_m$  is chosen empirically for stability. Separate diffusion coefficients could be used for the different materials (mud, gas, etc.). However, sufficient stability is obtained by only diffusing mud and salt using the same coefficient. This better preserves the accuracy of the location of gases and waste in the well.

Momentum is differenced as

$$V_i (\rho u)_i^* = V_i (\rho u)_i^{n-1} - \Delta t \left( A_{i+1/2} (\rho u)_{i+1/2}^{n-1} u_{i+1/2} - A_{i-1/2} (\rho u)_{i-1/2}^{n-1} u_{i-1/2} \right) - V_i \left( \frac{P_{i+1}^{n-1} - P_{i-1}^{n-1}}{2\Delta z} - \rho_i^{n-1} g + F_i^{n-1} \right) + \Delta t S_{mom,i} \quad (4.5.4)$$

where the dissipation term  $F_i^{n-1}$  is obtained from Eq. (4.1.7) and is constrained as follows:

$$\left| F_i^{n-1} \right| \leq \left| \frac{P_{i+1}^{n-1} - P_{i-1}^{n-1}}{2\Delta z} - \rho_i^{n-1} g \right| \quad (4.5.5)$$

and the sign  $F_i^{n-1}$  is chosen such that it opposes flow.

Finally, numerical momentum diffusion is added without distinguishing between phases in the mixture ( $\rho$  is the mixture density).

$$V_i (\rho u)_i^n = V_i (\rho u)_i^* - \zeta_p \Delta x_i \left[ A_{i+1/2} \left( (\rho u)_{i+1}^{n-1} - (\rho u)_i^{n-1} \right) - A_{i-1/2} \left( (\rho u)_i^{n-1} - (\rho u)_{i-1}^{n-1} \right) \right] \quad (4.5.6)$$

#### 4.6 Numerical Method – Repository

The time integration method for the repository flow is implicit, with spatial derivatives determined after the time increment. This method requires the inversion of a matrix for the entire repository, which is usually straightforward. The implicit scheme is unconditionally stable. However, it is still necessary to use small time steps to ensure gradient accuracy.

We start with Eq. (4.3.4), and employ the method described by Press et al. (1989). The equations presented below are for constant zone size. DRSPALL actually implements difference equations that allow for a variable zone size. Near the cavity, a small, constant zone size is used, and then zones are allowed to grow geometrically as the outer boundary is approached. This procedure greatly increases computational efficiency without sacrificing accuracy in the region of interest.

First, expand Eq. (4.3.4)

$$\frac{\partial \psi}{\partial t} = D(\psi) \left[ \frac{\partial^2 \psi}{\partial r^2} + \frac{(m-1)}{r} \frac{\partial \psi}{\partial r} \right] \quad (4.6.1)$$

Then, difference, treating  $D(\psi)$  as relatively constant over a zone, using its zone-centered value at the current time.

$$\frac{\psi_j^{n+1} - \psi_j^n}{\Delta t} = \frac{D_j^n}{\Delta r} \left[ \frac{\psi_{j+1}^{n+1} - 2\psi_j^{n+1} + \psi_{j-1}^{n+1}}{\Delta r} + \frac{(m-1)(\psi_{j+1}^{n+1} - \psi_{j-1}^{n+1})}{2r_j} \right] \quad (4.6.2)$$

Now, rearrange, collecting similar terms in  $\psi$ .

$$-\alpha_1 \psi_{j-1}^{n+1} + (1 + 2\alpha) \psi_j^{n+1} - \alpha_2 \psi_{j+1}^{n+1} = \psi_j^n \quad j=1,2,\dots \quad (4.6.3)$$

where

$$\alpha = \frac{D_j^n \Delta t}{(\Delta r)^2}$$

$$\alpha_1 = \left( \frac{D_j^n}{\Delta r} \right) \left( \frac{1}{\Delta r} - \frac{(m-1)}{2r_j} \right) \Delta t$$

$$\alpha_2 = \left( \frac{D_j^n}{\Delta r} \right) \left( \frac{1}{\Delta r} + \frac{(m-1)}{2r_j} \right) \Delta t$$

Eq. (4.6.3) is a tridiagonal system that may be solved by simplified LU decomposition as presented in Press (1989).

#### 4.6.1 Boundary Conditions.

The boundary condition at the inner radius is implemented by noting that for  $i = 1$  (the first intact or non-fluidized cell),  $\psi_{i-1}$  is the cavity pseudo pressure, which is known and, therefore, can be moved to the right hand side of Eq. (4.6.3).

$$(1 + 2\alpha) \psi_1^{n+1} - \alpha_2 \psi_2^{n+1} = \psi_1^n + \alpha_1 \psi_{cav}^{n+1} \quad (4.6.4)$$

The far field boundary condition is a zero gradient, which is implemented by setting  $\psi_{j+1}^{n+1} = \psi_j^{n+1}$  in Eq. (4.6.3), recognizing that  $1 + 2\alpha = 1 + \alpha_1 + \alpha_2$  and rearranging, which gives

$$-\alpha_1 \psi_{j-1}^{n+1} + (1 + \alpha_1) \psi_j^{n+1} = \psi_j^n \quad (4.6.5)$$

where  $j$  is the index of the last computational cell.

#### 4.6.2 Repository Stress State.

Once pore pressure is known, evaluation of the repository stress state, Eqs. (4.3.13) and (4.3.14), is algebraic except for the integral in the seepage stress calculations in Eqs. (4.3.15) and (4.3.16). The integrals are evaluated using trapezoidal integration with trapezoids formed between the cell centers where pore pressure and stress components are evaluated. The first increment is over the half-cell between the cavity wall and the center of the first non-fluidized cell. Radii are evaluated at cell centers, except for the left side in the first increment, which is the cavity wall radius.

$$\int_{r_c}^{r_j} [p(r_j) - p_{ff}] r_j^{m-1} dr = \sum_{i=0}^j 0.5 ((p_{i-1} - p_n) r_{i-1}^{m-1} + (p_i - p_n) r_i^{m-1}) (r_i - r_{i-1}) \quad (4.6.6)$$

Where  $i=1$  is the first intact cell (non-fluidized);  $j$  is index of the cell for which stress components are being evaluated;  $r_j$  is radius to the center of cell  $j$ ;  $p_0$  is the cavity pressure;  $r_0$  is the radius of cavity cell next to the interface; and  $n$  is the index of the last computational cell.

### 4.7 Numerical Method – Coupling

The calculation of gas flux from the repository to the wellbore (eqs 4.2.6) requires the gas velocity at the cavity interface,  $u_{repos}$  (eqs. 4.3.24). The velocity is evaluated numerically as follows:

$$u_{repos} = \frac{k'_1}{\eta\phi} \left( \frac{p_1 - p_{cav}}{\Delta r_1} \right) \quad (4.7.1)$$

The mass of gas flowing from the repository to the cavity at the bottom of the wellbore is then evaluated from:

$$\Delta m_{cav} = \rho_{g(repos)} u_{repos} \phi A_{cav} \Delta t \quad (4.7.2)$$

#### 4.8 Time Step Determination

For the wellbore, which uses a conditionally stable explicit method, the Courant condition

$$ss_m \frac{\Delta t}{\Delta z} < constant \quad (4.8.1)$$

is the basis of time step determination, where  $\Delta z$  is the zone size and  $ss_m$  is the sound speed in the mud:

$$ss_m = \sqrt{\frac{1}{c_m \rho_m}} \quad (4.8.2)$$

The wellbore timestep is calculated by replacing the inequality in (4.8.1) with equality, solving for  $\Delta t$  using a user specified *constant* and finding the minimum over all computational cells

$$\Delta t = \min \left( constant \frac{\Delta z_i}{ss_{m_i}} \right) \quad (4.8.3)$$

Normally, the value of the *constant* is taken as 1.0 for the “standard” Courant condition. However, due to the addition of the numerical diffusion terms and the extreme conditions in the present problem, especially where mass feeds from the repository into the wellbore, *constant* might be much less than 1 for a stable solution and is found by trial and error. A value that produces stable results (free of cell-to-cell oscillations) will typically work across a range of model parameter values.

For the repository, which uses an unconditionally stable implicit method, a constant timestep would typically be specified by the user. DRSPALL actually implements the timestep selection as a user specified factor,  $F_{repos}$ , that is multiplied by the Courant criteria that would normally be used by an explicit algorithm.

$$\Delta t = \min \left( F_{rep} \frac{\Delta r_i^2}{\frac{k'_i}{\varphi} \left( \frac{\psi_i}{\mu_i} \right)^{1/2}} \right) \quad (4.8.4)$$

Where  $\Delta t$  is the minimum over all cells in the repository domain. Trial and error or convergence testing can be used to find a timestep factor (usually greater than 1) that gives suitable results and gradient definitions.

The final timestep used is the lesser of the wellbore-determined and repository-determined timestep.

## 5 FLOW CHART WITH FUNCTIONAL REQUIREMENTS MAP

The major flow and control logic for DRSPALL is presented in **Figure 5-1** in the form of a flow chart. In the flow chart subroutine names are underlined and descriptive information is in 'Sentence case'. Also shown in the figure is a mapping of Functional Requirements. The requirement numbers (i.e., R.1) corresponds to those presented in the *Requirements Document* and summarized in Appendix A. Figure 5-1 shows the overall flow logic of DRSPALL and roughly corresponds to the DRSPALL main routine. Subsequent figures show details of modules that are first introduced in pentagonal elements in earlier figures. The modules (groups of subroutines) detailed in **Figures 5-2** through **5-4** are:

- DRSPALL – main program , input and initialization
- RunLoop – main calculational control including time-stepping loop
- CalculateWellBoreFlow – controls and calculates multi-component fluid flow in the wellbore and fluidization of failed waste.
- CalculateWasteFlow – controls and calculates gas flow through the waste in the repository and fluidization of the failed waste
- CalculateWasteStress – controls and calculates the effective stresses and spalling (tensile) failure in the waste

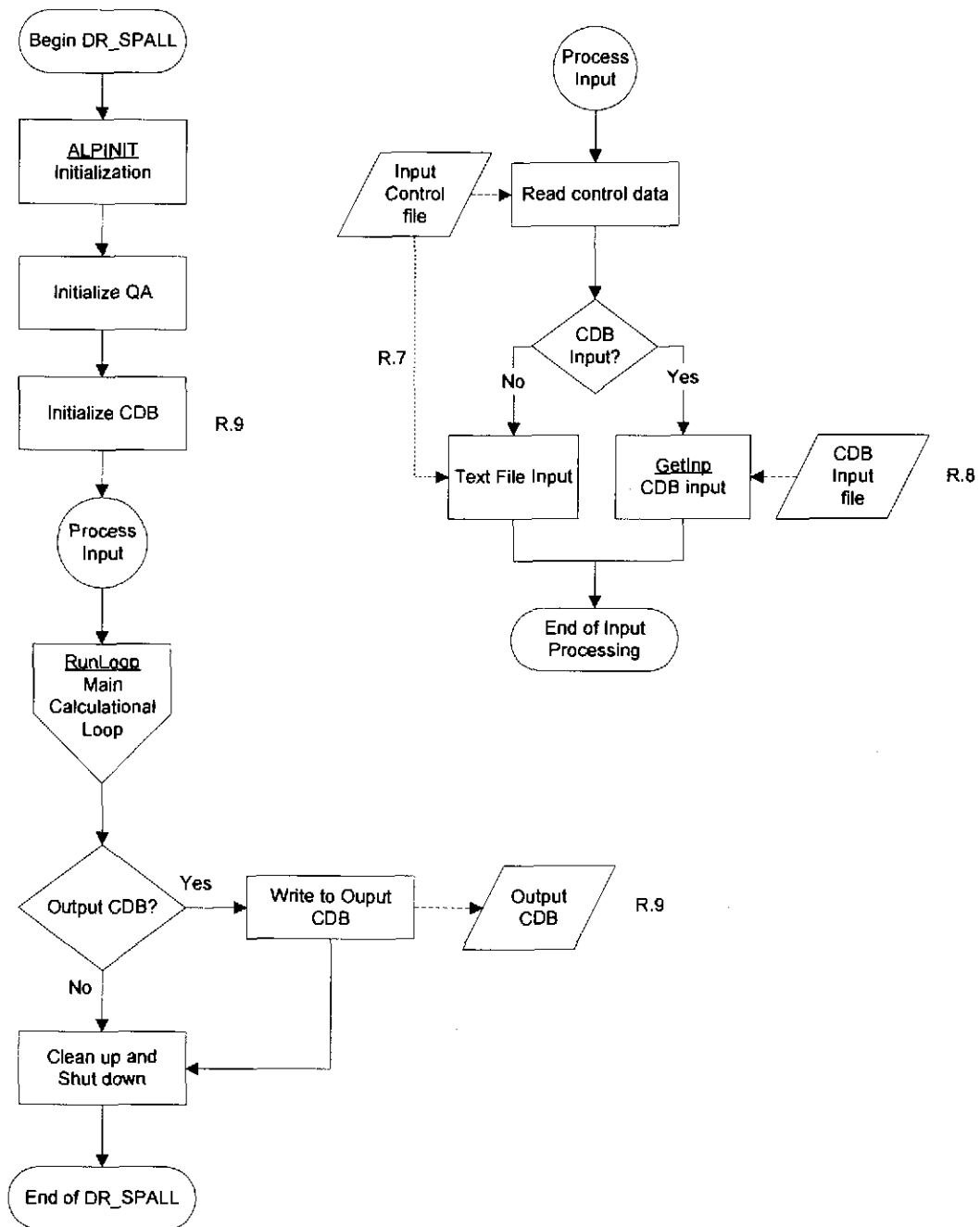


Figure 5-1. Flow Chart for Program DRSPALL

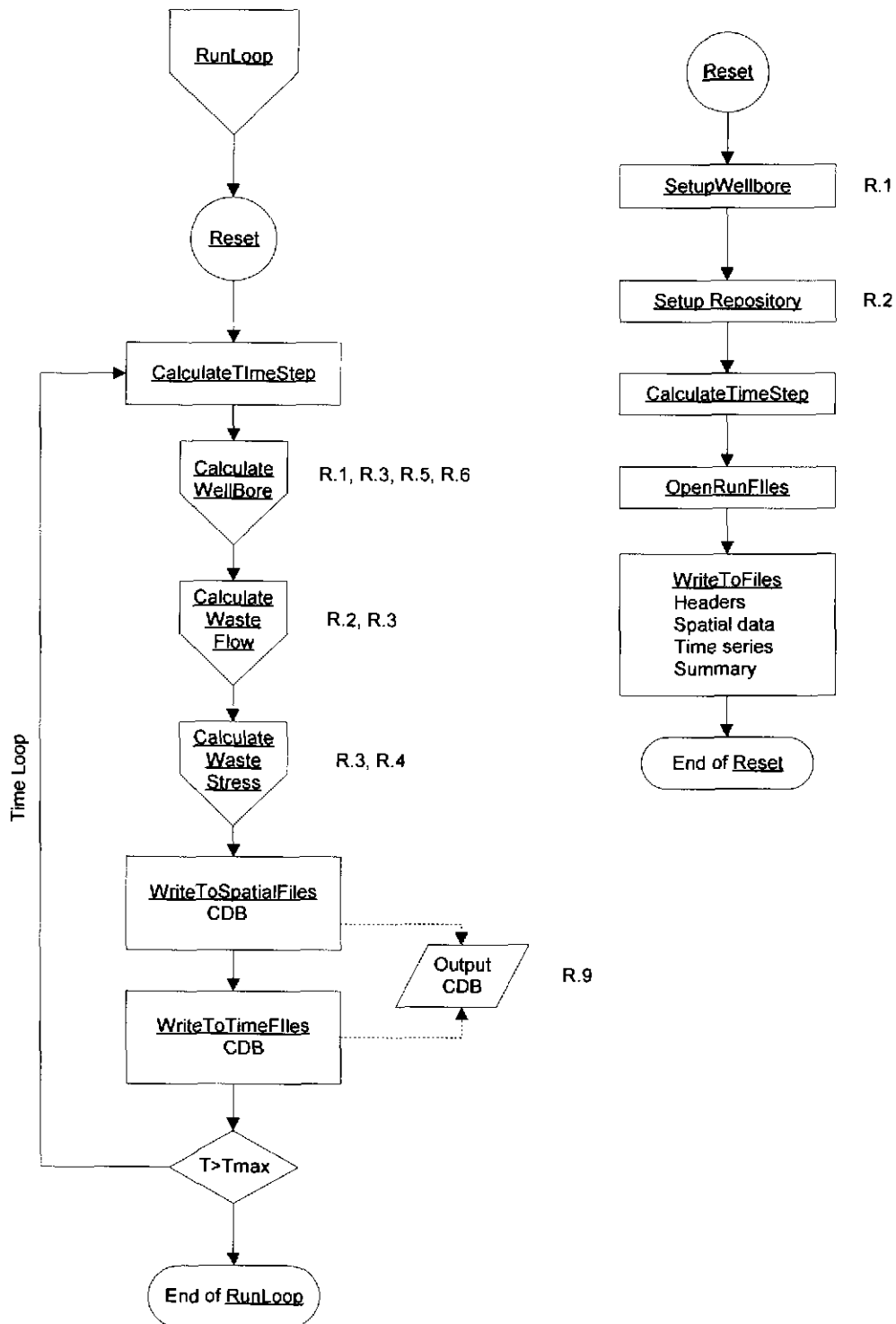


Figure 5-2. Flow Chart for Subroutine RunLoop

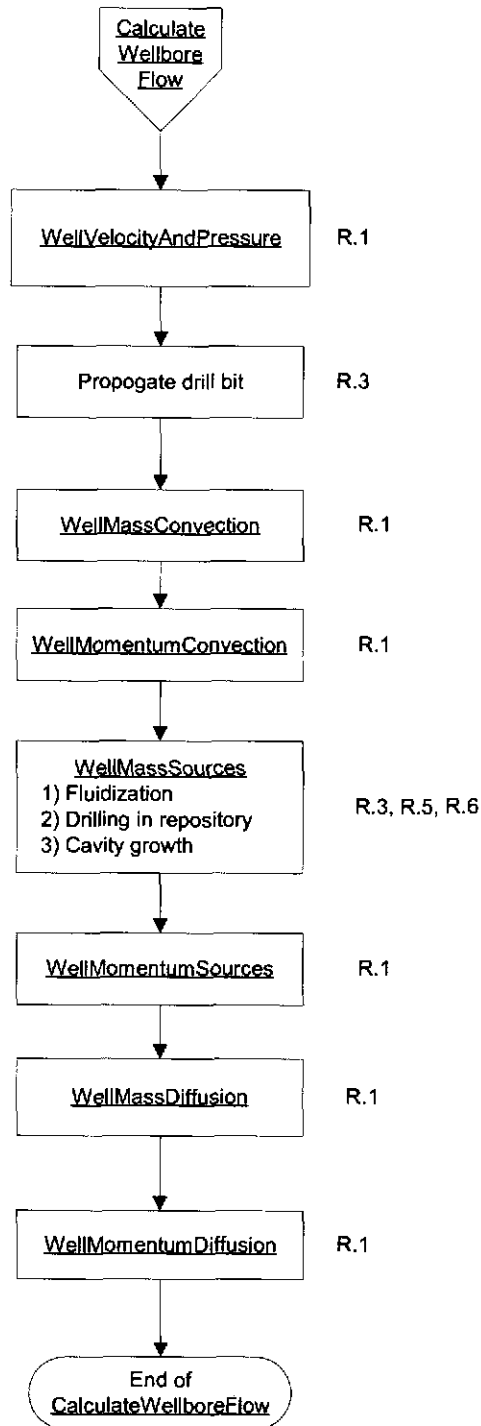


Figure 5-3. Flow Charts for Subroutines CalculateWellBoreFlow

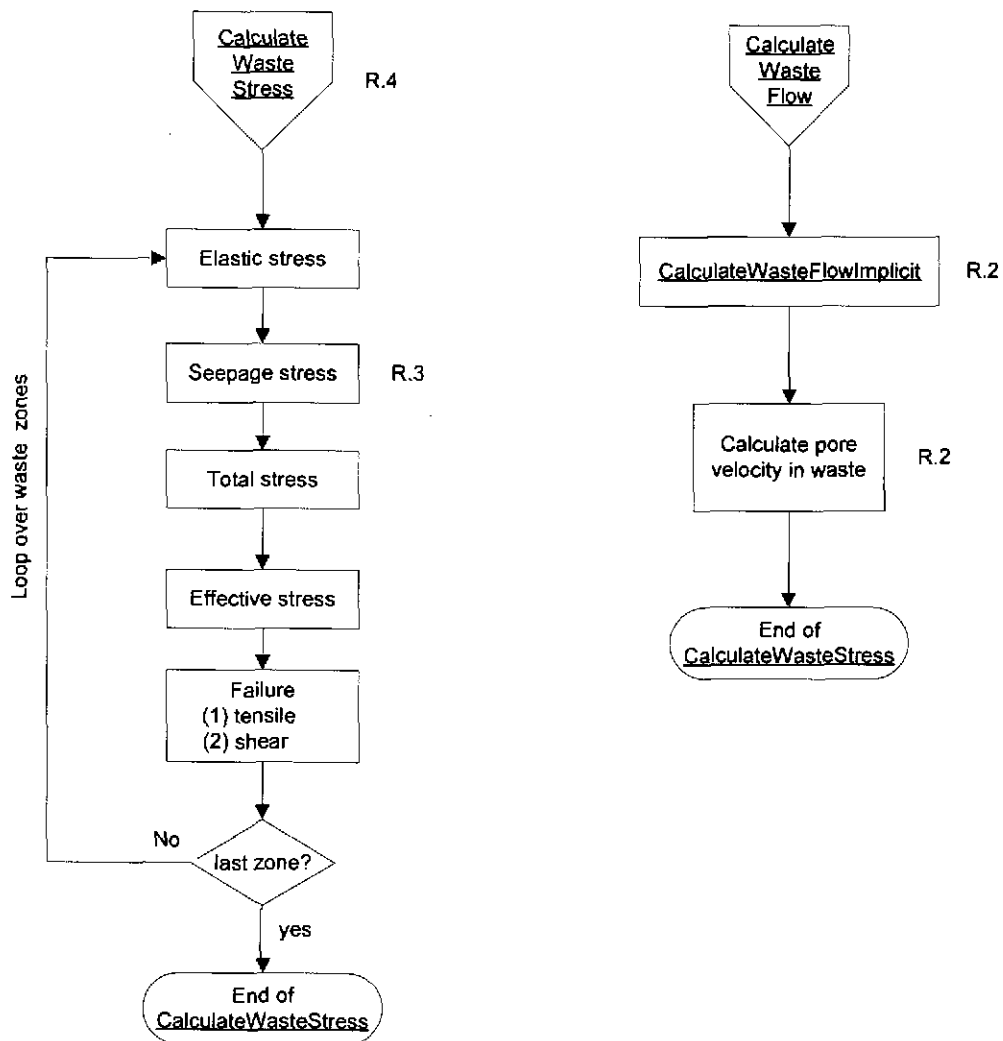


Figure 5-4. Flow Chart for Subroutine CalculateWasteStress and CalculateWasteFlow

## 5.1 Call Tree With Subroutine Descriptions

The following is the DRSPALL call tree that includes a brief routine (subroutine or function) description. An indentation indicates a call to the named routine. The combination of the flow charts in Section 5.1 and the following call tree provides a complete description of the DRSPALL flow logic

DRSPALL	Main program
. ALPINIT	Initialization
. . ReadControlFile	Read input control parameters, properties from control file or input CAMDAT file
. . CheckParameterBounds	Checks that input parameters are within valid range
. . InitializeTextOutput	Opens output files and writes headers
. . Reset	Problem setup control
. . . SetupWellbore	Setup wellbore flow model
. . . . ZoneWellbore	Setup grid in wellbore
. . . SetupRepository	Setup Repository waste model
. . . . CalculateWasteStresses	Initialize stress in repository
. . . CalculateTimestep	Calculate initial time step
. . . SetSpatialSaveTimes	Setup times for saving spatial variables
. . . SetTimeSaveTimes	Setup times for saving time series data
. . . OpenRunFiles	Open output text files
. . . WriteFileHeaders	Write header record to output files
. . . CloseRunFiles	If calculation finished, close files
. . CreateCDBHeader	Initializes and output CAMDAT file
. . CreateCDBVariables	Defines output variables for output CAMDAT file
. RunLoop	Calculation control

### *Begin Time Loop*

. . CalculateTimestep	Calculate time increment for current step
. . CalculateWellboreFlow	Wellbore flow model control
. . . WellVelocityAndPressure	Fluid velocity and pressure in wellbore
. . . WellMassConvection	Mass flow (balance) in wellbore
. . . WellMomentumConvection	Momentum balance in wellbore
. . . WellMassSources	Determine mass sources (mud, gas, waste...)
. . . WellMomentumSources	Determine momentum sources
. . . WellMassDiffusion	Mass diffusion
. . . WellMomentumDiffusion	Momentum diffusion
. . CalculateWasteFlow	Gas flow in repository control

- . . . CalculateWasteFlowImplicit    Implicit solver for gas flow in repository
- . . CalculateWasteStresses        Effective stress model with seepage forces
- . . OutputControl                  Controls output to text and CAMDAT files

*End of time loop*

- . . RunShutDown                    Clean up for termination

DRSPALL is written in FORTRAN 90 for compilation under OpenVMS on the WIPP Alpha cluster, but is designed to be relatively portable. The subroutines and functions that make up DRSPALL have been logically grouped by functionality into the compilable FORTRAN 90 (.f90) source files that follows:

CDBControl.f90	Collection of routines that read from and write to CAMDAT files.
CDBGlobals.F90	Global variables related to CAMDAT files are declared here
DRSPALL.F90	This is the main program source file, which includes input control and initialization, QA functions and CAMDAT file initialization.
FILEWRITE.F90	Collection of subroutines that write data to the output text file.
GLOBALS.F90	Global variables are declared here.
MAINCALC.F90	Collection of subroutines that include the main run loop and timestep calculations
PARAMETERS.F90	Collection of subroutines that control parameter initialization and writes to the input parameter data echo.
SETUPCALC.F90	Collection of subroutines that initialize the wellbore, repository and other values required to start a run.
WASTEFLOWCALC.F90	Collection of subroutines that calculate pressure and fluid flow in the repository.
WATESTRESSCALC.F90	Subroutine that calculates solid stresses and failure in the repository.
WELLBORECALC.F90	Collection of subroutines that calculate fluid flow in the well, including pumping, expulsion and the coupling to the repository via the DDZ or cavity.

## 6 DATA STRUCTURES (I/O)

The primary data structures used by DRSPALL are the input files, output files and two FORTRAN 90 modules that contain most of the problem variables and parameters that must be shared between subroutines. Each of these structures is detailed in the following subsections.

Files are named with the prefix of the run name provided by the user and are suffixed according to the data contained in the file. The suffix and the corresponding data file description are summarized in **Table 6-1**.

*Table 6-1. Summary of DRSPALL Input and Output Files.*

Suffix	File contents
DRS	Input control and problem specification parameters
CDB	Input and output CAMDAT Database files
DBG	Input data echo and runtime diagnostics

### 6.1 Input Files

#### 6.1.1 Input Control and Parameter File

The input control and parameter file, suffixed 'DRS', lists input control and problem specification parameters. The following problem specification parameters are specified in this file:

Land Elevation	Particle Diameter
Repository Top	Gas Density at STP
Total Thickness	Gas Viscosity
DRZ Thickness	Mud Density
DRZ Permeability	Mud Viscosity
Outer Radius	Wall Roughness, Pipe
Initial Gas Pressure	Wall Roughness, Annulus
Far-Field In-Situ Stress	Max. Solids Vol. Fraction
Porosity	Solids Viscosity Exponent
Permeability	Choke Efficiency
Forchheimer Beta	Bit Diameter
Biot Beta	Pipe Diameter
Poisson's Ratio	Collar Diameter
Cohesion	Pipe Inside Diameter
Friction Angle	Collar Length
Tensile Strength	Exit Pipe Length
Characteristic Length	Exit Pipe Diameter

Drilling Rate	Stop Pumping Exit Velocity
Bit Above Repository (Initial)	Stop Drilling Time
Mud Pump Rate	Spherical/Cylindrical Geometry Flag
DDZ Thickness	Fluidization Flag
DDZ Permeability	Maximum Run Time
Stop Drilling Exit Velocity	Repository Cell Length
	Repository Cell Growth Rate
	Wellbore Cell Length
	Wellbore Cell Growth Rate

### 6.1.2 *Input CDB File*

The user will be able to optionally read the problem specification data listed in Section 6.1.1 from an input CDB file. The details of the self-describing file structure can be found in Rechar et al (1993) and in the *WIPP PA Users Manual for CAMDAT\_LIB* (WIPP 1996a). CAMDAT\_LIB provides a simplified programmers interface for accessing the data contained in a CDB file through subroutine calls.

## 6.2 **Output Files**

### 6.2.1 *Output Text Files*

A single output text file is created (suffix .DBG) which contains

- An echo of the input .DRS file.
- A listing of the input parameters, after processing, that reflects the actual parameters used in the current analysis. This includes values of parameters that were retrieved from the input CAMDAT file.
- A several line summary of results and timing information for each timestep that data is written to the output CAMDAT file.
- Run time diagnostic messages.
- A results summary at the end of the calculation.

### 6.2.2 *CDB Output File*

The optional CDB output file will contain, at a minimum, all input problem specification parameters listed in Section 6.1.1 and all the output data listed in Section 6.2.1. The CDB file is flexible enough to handle both spatial and temporal variables. The self-describing file structure is documented Rechar, (1993) and the *WIPP PA Users Manual for CAMDAT\_LIB* (WIPP 1996a). CAMDAT\_LIB provides a simplified programmers interface for creating the CDB file through subroutine calls.

### 6.3 FORTRAN 90 Global Variables Modules

Two FORTRAN 90 modules (*globals.f90*, *CDBglobals.f90*) have been defined for specifying all global variables. *CDBglobals.f90* contains shared variables related to reading and writing CAMDAT files. *Globals.f90* contains all other shared variables. The modules include variable type declarations (integer, real, character, logical), precision (double, single), array dimensioning, records, structures definitions and parameter value setting. All the information contained in the module is made accessible to a routine by including a “*USE globals*” or “*USE CDBglobals*” statements in the declaration section of the routine. This is typically the first executable statement in the routine. DRSPALL uses variable names that are self-descriptive and therefore, the *globals.f90* and *CDBglobals.f90* listing shown below are, essentially, self-documenting. Note that some of the lines maybe wrapped.

```

!-----
!
! File Globals.f90 -- contains global parameters, variables, and constants
!
!-----

Module Globals

!Use DFWin
!Use DFLib
!Use GraphicsRecords
Implicit NONE

! Input Parameters
! -----

! Repository
Real(8) surfaceElevation, repositoryTop, repositoryThickness, drZThickness, &
  drZPerm, uncompactedWastePorosity, repositoryHeight, repositoryThickness0, &
  repositoryOuterRadius, repositoryInitialPressure, farFieldPorePressure, &
  farfieldStress, reposRadius1, growthRate

! Waste
Real(8) repositoryInitialPorosity, repositoryInitialPerm, forchBeta
Character(1) permFromPorosity
Real(8) biotBeta, poissonsRatio, cohesion, frictionAngle, tensileStrength, &
  particleDiameter, fluidizationVelocity, Lt

! Gas
Real(8) gasBaseDensity, gasViscosity

! Mud
Real(8) initialMudDensity, mudViscosity, wallRoughness(2), mudSolidsMax, &
  mudSolidsViscosityExponent

! Wellbore/Drilling
Real(8) bitDiameter, pipeDiameter, collarDiameter, pipeInsideDiameter, collarLength, &
  drillingRate, initialBitAboveRepository, mudPumpRate, dDZThickness, dDZPerm, &
  stopDrillingExitVolRate, stopPumpingExitVolRate, stopDrillingTime, timeToFloor, &
  maxPumpPressure, initialPumpRate, pitGain

! Computational
Character(1) numericalMethod, geometry, allowFluidization, frictionModelName
Real(8) maxTime, initialReposZoneSize, initialWellZoneSize, &
  wellStabilityFactor, reposStabilityFactor

! APG Plot axes minimums / maximums (left here for compatibility with PC version)
Real(8) minPlotRadius, maxPlotRadius, minPlotWellPos, maxPlotWellPos, &
  minPlotPressure, maxPlotPressure, minPlotStress, maxPlotStress, &
  minPlotVelocity, maxPlotVelocity, &
  minPlotWellPressure, maxPlotWellPressure, &
  minPlotWellVelocity, maxPlotWellVelocity, &
  minPlotWellRho, maxPlotWellRho, &
  minPlotWellFraction, maxPlotWellFraction
Logical newPlotRadius, newPlotWellPos, &
  newPlotPressure, newPlotStress, newPlotVelocity, &
  newPlotWellPressure, newPlotWellVelocity, newPlotWellRho, newPlotWellFraction

! Internal Parameters and Variables
! -----

! Repository array
Logical(1) , DIMENSION(:), ALLOCATABLE :: &
  tensileFailureStarted, tensileFailureCompleted, shearFailed, &
  fluidizationStarted, fluidizationCompleted
REAL(8), DIMENSION(:), ALLOCATABLE :: &
  reposRadius, reposRadiusH, reposPres, porosity, permeability, forchratio, &
  poreVelocity, superficialVelocity, reposFactor, pL, &
  psi, dCoeff, radEffStress, tanEffStress, shearStress, &
  fractionTensileFailed, tensileFailureTime, meanEffStress, shearStrength, &

```

```

fractionFluidized, fluidizationTime, FluidStartTime, FluidStopTime, FailStartTime, &
radElasticStress, tanElasticStress, radSeepageStress, tanSeepageStress, &
reposDR, reposDRH, reposVol, reposGasMass, drillingFailure
Real(8) , DIMENSION(:), ALLOCATABLE :: aa, bb, cc, rr, gam

! Repository non-array
Integer(2) geomExponent
Integer(4) numReposZones, maxTensileFailedIndex, maxShearFailedIndex, firstIntactZone, &
frictionModel, interfacel, interface2, lastFailedZone, firstInternalFailedZone
Real(8) reposZoneSize, wasteBoundaryPoreVelocity, sumReposGasMass, &
totalGasFromWaste, totalWasteFromRepos

!JFS3
Integer(4) fluidizationWaitZone
Logical(1) surfaceFailureAllowed

! Cavity
Real(8) cavityPres, initialCavityRadius, initialCavityArea, initialCavityVol,
initialCavityGasVol, &
cavityGasMass, cavityWasteVol, cavityWasteMass, deltaGasIntoWell, deltaWasteIntoWell, &
deltaSaltIntoWell, deltaGasFromWaste, exitPoreVelocity, exitPoreArea

! Wellbore array
REAL(8), DIMENSION(:), ALLOCATABLE :: &
wellPos, wellPres, wellRhoV, wellVol, WellArea, wellZoneSize, &
wellLV, wellRho, wellAreaInt, wellDeltaVInt, wellFactor, &
wellMudMass, wellGasMass, wellWasteMass, wellSaltMass, &
wellMudVol, wellGasVol, wellWasteVol, wellSaltVol, hydraulicDia
REAL(8), DIMENSION(:), ALLOCATABLE :: &
wellMassOrig, wellPresOrig, wellMudMassOrig, &
wellGasMassOrig, wellWasteMassOrig, wellSaltMassOrig
REAL(8), DIMENSION(:), ALLOCATABLE :: &
wellGRhoStar, wellGRhoVStar, wellGRhoT, wellGRhoVT, &
wellVolInt, momDiff, massDiff

! Wellbore non-array
Logical(1) repositoryPenetrated, firstPenetration, drilling, pumping, exitPipe, &
internalFailure

Integer(4) numWellZones, wellBottomIndex, numExitZones, firstWellZone, &
numWellZones1, numWellZones2, numWellZones3, numWellZones4

Real(8) wellLength, bitAboveRepository, dRZDiameter, dRZArea, wellGrowthRate, &
bitArea, bitFlowArea, pipeArea, collarAnnulusArea, pipeAnnulusArea, &
exitPipeLength, exitPipeDiameter, exitPipeArea, wellDepth, &
mudMassEjected, gasMassEjected, wasteMassEjected, saltMassEjected, &
totalMudInWell, totalGasInjected, totalGasInWell, totalWasteInWell, totalSaltInWell, &
cuttingsMassMax, cuttingsRadiusMax, equivDrilledCavityRadius, &
volStore, wasteStore, gasStore, wasteInjected, originalBitDiameter, &
sumWellGasMass, cutVol, splVol, TotVol, cutTrueVol, &
sumWellWasteMass, Z1, Z2, Z3, Z4

! General array
REAL(8), DIMENSION(:), ALLOCATABLE :: invPorosity

! General non-array
Real(8) invGasViscosity, invWellZoneSize, invWasteDensity, invSaltDensity,
invWaterCompressibility, &
invInitialMudDensity, invGasBaseDensity, invInitialCavityGasVol, invPi,
invAtmosphericPressure, &
invReposZoneSize, timeOfPenetration

! Computational Parameters and Constants
!-----

! Run management
Real(8) runTime, deltaTime
Real cpuTime, cpuBegin, cpuEnd
Integer(4) runIndex
Logical(1) stopRun, isRunning, pauseRun, CDBOutput, textOutput

```

Character\*3 platform, machine  
Character\*132 root

```

! Window unit constants
Integer(4) ParameterUnit, TimeUnit, RepositorySpatialPressureUnit,
RepositorySpatialStressUnit, &
  RepositorySpatialVelocityUnit, WellboreSpatialPressureUnit, WellboreSpatialMassUnit, &
  ResultsSummaryUnit

! File logic
!Type(T_OpenFilename) fName
!Logical(1) fileLoaded, fileSaved, fileNameed
Character(255) fullParameterFilename, pressureFileName, radEffStressFileName, &
  tanEffStressFileName, poreVelocityFileName, timeFileName, summaryFileName,
  outParamsFileName,&
  diagnosticFileName, TC1chanFileName, TC4couplefilename, TC4stressfilename, &
  TC4Fluidfilename, TC4Ejectfilename, TC5Wellfilename

Integer(4) parameterFileID, pressureFileID, radEffStressFileID, tanEffStressFileID, &
  poreVelocityFileID, timeFileID, summaryFileID, outParamsFileID, diagnosticFileID, &
  chanValidationFileID, &
  !test case #4
  couplingValidationFileID, stressValidationFileID, fluidizationvalidationFileID, &
  expulsionValidationFileID, &
  !test case #5
  wellboreValidationFileID

! Character-based user input parameter values
Character(30) gridItems(2,44)
Character(10) gridUnits(2,44)
Character(14) gridValues(2,44)

! Parameter input grids
Integer(2) numGridRows, numGridCols, rowHeight, margin
Integer(2) gridWidth, colWidth(3)

! DKR Graphics records moved to separate module for portatibility with VMS

! Plot and save times
Real(4) spatialPlotTime(1000), spatialSaveTime(0:1000), &
  timeSaveTime(0:2000), &
  radius1, radius2, radius3, chanSaveTime(10)
Integer(4) spatialPlotIndex, spatialSaveIndex, timeSaveIndex, &
  ncount1, ncount2, ncount3, chanSaveIndex

! APG for time plots
Integer ixtplt
Real(4) finaltplt
Integer, Parameter :: maxtplt = 1000
Real(4) tpltTime(0:maxtplt)
Real(4) tpltPumpPressure(0:maxtplt), tpltWellBottomPressure(0:maxtplt),
tpltCavityPressure(0:maxtplt), &
  tpltDrilledRadius(0:maxtplt), tpltCavityRadius(0:maxtplt), tpltTensileRadius(0:maxtplt), &
  tpltWasteBoundaryPoreVelocity(0:maxtplt), tpltFluidizationVelocity(0:maxtplt),
tpltMudEjectionVelocity(0:maxtplt), &
  tpltWasteInWell(0:maxtplt), tpltWasteEjected(0:maxtplt), &
  tpltGasInjected(0:maxtplt), tpltGasInWell(0:maxtplt), tpltGasEjected(0:maxtplt), &
  tpltGasPosInWell(0:maxtplt), tpltWastePosInWell(0:maxtplt)

! for plotting and saving
! time plots
Real(4) curTime, &
  curPumpPressure, curWellBottomPressure, curCavityPressure, &
  curDrilledRadius, curCavityRadius, curTensileRadius, &
  curWasteBoundaryPoreVelocity, curFluidizationVelocity, curMudEjectionVelocity, &
  curWasteInWell, curWasteEjected, &
  curGasInjected, curGasInWell, curGasEjected, &
  curGasPosInWell, curWastePosInWell

Real(4) prevTime

```

```

Real(4) prevPumpPressure, prevWellBottomPressure, prevCavityPressure, &
  prevDrilledRadius, prevCavityRadius, prevTensileRadius, &
  prevWasteBoundaryPoreVelocity, prevFluidizationVelocity, prevMudEjectionVelocity, &
  prevWasteInWell, prevWasteEjected, &
  prevGasInjected, prevgasInWell, prevGasEjected, &
  prevGasPosInWell, prevWastePosInWell

! summary display
Real(4) displayedTime, &
  displayedPumpPressure, displayedBitAbove, &
  displayedWellBottomPressure, displayedCavityPressure, displayedWasteBoundaryPoreVelocity, &
  displayedFluidizationVelocity, displayedEquivDrilledCavityRadius, displayedCavityRadius, &
  displayedTensileFailedRadius, displayedShearFailedRadius, displayedGasInjected, &
  displayedMudInWell, displayedGasInWell, displayedWasteInWell, displayedSaltInWell, &
  displayedMudVelocity, displayedMudVolRate, displayedMudEjected, displayedGasEjected,
  displayedWasteEjected, displayedSaltEjected, &
  displayedMudExitFraction, displayedGasExitFraction, displayedWasteExitFraction,
  displayedSaltExitFraction, &
  displayedGasPosInWell, displayedWastePosInWell, displayedradEffStress,
  displayedFirstIntactZone

Integer cellControl(5), oldCellControl, stepControl, oldStepControl
Integer DisplayedCell
Character*8 stepControlName(5), displayedControl

! Validation Test Case specific parameters
Integer(2) validationTestCase, validationSubcase
Real(8) characteristicTime

!test case #4
Real(8) stressSaveTime, stressSaveDelta, fluidizationSaveTime, fluidizationSaveDelta, &
  initialGasInRepository

!DKR - parameters switched to variables. set in reset
REAL(8) gravity, MassDiffusionFactor, MomentumDiffusionFactor, chokeEfficiency, &
  WaterCompressibility, GasConstant, ReposTemp, WasteDensity, saltDensity, &
  BitNozzleNumber, BitNozzleDiameter, Pi, AtmosphericPressure, shapeFactor, &
  TensileVelocity

Integer(2) FIX, ENG

! Constants
Integer(2), Parameter :: FULL_RESET = 1
Integer(2), Parameter :: RUNNING = 2
Integer(2), Parameter :: REOPENING = 3

end

```

## MODULE CDBGlobals

```

!-----
! This module conatins variables required to read or write a CDB
!
! By: David Rudeen
! GRAM, Inc.
!
! Modification History
! 12/19/02 - DKR: Original version
!-----
IMPLICIT NONE
INTEGER, PARAMETER :: nev=26, nhv=47
CHARACTER*8 HisName(nhv), NAMXYZ(3), EleName(nev), blockName
CHARACTER*80 HEAD

```

```

CHARACTER*255 outCDBFilename, inCDBFilename
INTEGER      IDBout, NOUT, NumHisVar, LDUM, IERRDB, NDIM, NUMNP, &
              NELBLK, NELX, NELY, NELZ, MAXLNK, NEB, NUMPRP, NUMATR, &
              NUMEL, NumEleVar, outCDBFileID, inCDBFileID, &
              NINFO, numCDBsteps, numParam
INTEGER      IDBin, NQAREC, NELBLKin, NUMATRin, NUMPRPin, NUMNPS, LNPSNL, &
              NUMESS, LGELEL, LGNODL, DRSblock, reposBlock, wellBlock1, wellBlock2
LOGICAL,     DIMENSION(:, :), ALLOCATABLE :: ISEVOK, ISPROK
LOGICAL,     DIMENSION(:),   ALLOCATABLE :: ISATOK
INTEGER,     DIMENSION(:, :), ALLOCATABLE :: Link
INTEGER,     DIMENSION(:),   ALLOCATABLE :: EleMap, IDELB, NUMLNK, NUMELB
REAL(4),     DIMENSION(:),   ALLOCATABLE :: Xn, Yn, ELEVAT, THICK, DEL_Y, DEL_X
REAL(4),     DIMENSION(:, :), ALLOCATABLE :: EleVal, PROP
CHARACTER*80, DIMENSION(:),   ALLOCATABLE :: INFO
CHARACTER*8 , DIMENSION(:),   ALLOCATABLE :: NAMELB, PRPname, ParamName, NAMATR
CHARACTER*8 , DIMENSION(:, :), ALLOCATABLE :: QAREC

REAL(4)      RMEM(1), HisVal(nhv), ZN(1)
CHARACTER*1  CMEM(1)
LOGICAL      WHOLE, CDBinput

END

```

## 7 PARAMETER RANGES

Many of the parameters must be within certain acceptable ranges to represent physical reality or true repository and/or wellbore conditions or for compatibility with other input parameters. Where possible, a limitation scheme involving parameter range checking at the time parameters are read in will flag unacceptable parameter values and stop execution. But, because DRSPALL has been designed for any self-consistent set of input parameters and any single parameter value can vary significantly depending on the system-of-units, it is not possible to provide upper bounds for many of the input parameters. **Table 7-1** list all input variables and provides parameter bounds when they can be reasonably defined.

*Table 7-1. Input Parameters and Ranges*

<b>Parameter Description</b>	<b>Range</b>
Land Elevation	> Repository Top
Repository Top	Any real
DRZ Thickness	> 0
DRZ Permeability	> 0
Outer Radius	> 0.5*bit diameter
Initial Gas Pressure	>0, < overburden ( $\rho_s g h$ ); h=Land Elevation – Repository Top
Far-Field In-Situ Stress	>0, < overburden
Porosity	0< porosity<1.0
Permeability	>0.
Permeability from Porosity Flag	Y or N
Biot Beta	$\geq 0, \leq 1$
Poisson's Ratio	0< Poisson's Ratio<0.5
Cohesion	> 0.
Friction Angle	0< Friction Angle < 90
Tensile Strength	< 0.
Particle Diameter	< Bit Diameter
Gas Density at STP	>0
Gas Viscosity	>0
Mud Density	>0
Mud Viscosity	>0
Wall Roughness	>0
Max. Solids Vol. Fraction	>0, <1
Solids Viscosity Exponent	<0
Bit Diameter	>0
Pipe Diameter	>0, <bit diameter
Collar Diameter	>pipe diameter, < bit diameter
Pipe Inside Diameter	>0, <pipe diameter
Collar Length	> 0, <h
Drilling Rate	>0,

<b>Parameter Description</b>	<b>Range</b>
Bit Above Repository (Initial)	>0, < h
Mud Pump Rate	>0
DDZ Thickness	>0
DDZ Permeability	>0
Stop Drilling Exit Velocity	>0
Stop Pumping Exit Velocity	>0
Explicit/Implicit	Y or N
Spherical/Cylindrical Geometry Flag	S or C
Fluidization Flag	Y or N
Maximum Run Time	> 0
Repository Cell Length	> 0
Wellbore Cell Length	> 0
Land Elevation	> Repository Top
Repository Top	Any real
DRZ Thickness	> 0
DRZ Permeability	> 0
Outer Radius	> 0.5*bit diameter
Initial Gas Pressure	>0, < overburden ( $\rho_s g h$ ); h=Land Elevation – Repository Top
Far-Field In-Situ Stress	>0, < overburden
Porosity	0< porosity<1.0
Permeability	>0.
Permeability from Porosity Flag	Y or N
Biot Beta	>=0, <=1
Poisson's Ratio	0< Poisson's Ratio<0.5
Cohesion	> 0.
Friction Angle	0< Friction Angle < 90
Tensile Strength	< 0.
Particle Diameter	< Bit Diameter
Gas Density at STP	>0
Gas Viscosity	>0
Mud Density	>0
Mud Viscosity	>0
Wall Roughness	>0
Max. Solids Vol. Fraction	>0, <1
Solids Viscosity Exponent	<0
Bit Diameter	>0
Pipe Diameter	>0, <bit diameter
Collar Diameter	>pipe diameter, < bit diameter
Pipe Inside Diameter	>0, <pipe diameter
Collar Length	> 0, <h
Drilling Rate	>0,
Bit Above Repository (Initial)	>0, < h

<b>Parameter Description</b>	<b>Range</b>
Mud Pump Rate	>0
DDZ Thickness	>0
DDZ Permeability	>0
Stop Drilling Exit Velocity	>0
Stop Pumping Exit Velocity	>0
Explicit/Implicit	Y or N
Spherical/Cylindrical Geometry Flag	S or C
Fluidization Flag	Y or N
Maximum Run Time	> 0
Repository Cell Length	> 0
Wellbore Cell Length	> 0

## 8 TEST CASE CONTROL LOGIC

Each of the validation test cases described in the DRSPALL Verification and Validation Plan / Validation Document (WIPP PA, 2003a), requires some code control logic specific to the test case. This involves either turning off functionality not required in the test case, setting special boundary conditions, or creating formatted ASCII output files that are analyzed and evaluated against the acceptance criteria outlined in the VVP/VD. The input control file to DRSPALL contains a parameter that identifies the specific test case running, i.e., "1.2." The subsequent discussion identifies the code logic specific to these test cases, and includes rationale for why the logic is used.

The following nomenclature is used in this section:

*Table 8-1. Nomenclature for Section 8 - Test Case Control Logic .*

<b>Symbol</b>	<b>Definition</b>	<b>Units</b>
$a$	Cavity radius	m
$A$	Surface area of cavity forming interface between repository domain and wellbore domain	m <sup>2</sup>
$D_b$	True diameter of drill bit	m
$D_E$	Effective diameter of drill bit required to simulate full penetration at early time for the porous flow test problem	m
$\eta$	Gas viscosity	Pa·sec
$H$	Height of repository at time of penetration	m
$k$	Repository permeability	m <sup>2</sup>
$\phi$	Repository porosity	--
$P(r)$	Gas pressure as a function of radius at a given time	Pa
$P_1$	Initial repository pressure	Pa
$\tau$	Dimensionless time	--
$t_o$	Characteristic time	sec
$t$	Time	sec
$\Psi$	Dimensionless pseudopressure	--
$z$	Dimensionless radius	--
$\zeta$	Dimensionless plotting parameter	--

## 8.1 Porous Flow Test Problem

The purpose of the gas flow test problem is to determine whether DRSPALL can accurately calculate transient gas pressures in the repository during the first few seconds after a borehole intrusion. The problem is designed to simulate the repository domain only. As such, the wellbore domain is decoupled from the repository and inactive during execution of the test problem. Input parameters pertaining to the wellbore are therefore irrelevant in this test case, as are any code output describing wellbore conditions.

### 8.1.1 Constant pressure inner boundary

The test problem calls for a constant pressure inner boundary. While normal execution of DRSPALL couples the repository and wellbore with a common pressure boundary, this test case circumvents the coupling by assigning an inner boundary gas pressure of  $P = 0$  MPa.

### 8.1.2 Effective bit diameter

Drilling does not actually progress in this test case. Rather, the problem starts with a “cavity” cut out of the repository that has a surface area equivalent to the area of the cavity face that would result from the penetration of the true bit diameter  $D_b$  through a repository of height  $H$ . The surface area  $A$  of this cylinder representing the borehole wall is evaluated as:

$$A = \pi D_b H \quad (8.1.1)$$

where the flat ends of the cylinder are not considered because these do not transfer gas between the repository and the wellbore at full penetration. For the purpose of this test case, an effective bit diameter  $D_E$  must be defined that represents a hypothetical bit that creates a cavity of area  $A$  the instant it touches the repository. The initial contact geometry of the bit with the repository is a circle, with diameter  $D_E$ . The effective diameter is therefore related to the cavity area by the formula for the area of a circle:

$$A = \frac{\pi D_E^2}{4} \quad (8.1.2)$$

Setting the surface areas in Eqs. 8.1.1 and 8.1.2 equal to one another yields:

$$A = \frac{\pi D_E^2}{4} = \pi D_b H \quad (8.1.3)$$

and rearranging to solve for  $D_E$  yields:

$$D_E = 2\sqrt{D_b H} \quad (8.1.4)$$

The effective diameter is calculated by the code only if this test case flag is turned on. While the actual bit diameter  $D_b$  is read as an input variable for this test case,  $D_E$  is calculated according to Eq. 8.1.4 and used in the porous flow calculations.

The cavity radius,  $a$ , used for the characteristic time shown in Table 8-2 below, is defined depending on the problem geometry. For the cylindrical case,  $a$  is equal to the true bit radius:

$$a = D_e/2 \quad (8.1.5)$$

and for the spherical case,  $a$  is defined as the radius of a hemisphere with area  $A$ :

$$a = \sqrt{\frac{A}{2\pi}} \quad (8.1.6)$$

### 8.1.3 Special output and dimensionless variables

The methodology outlined in Chan et al. (1993) calls for the definition of several special variables defined in Table 8-2.

**Table 8-2. Special variables defined for Porous Flow Test Problem**

Variable name	Definition	Eq. number
Dimensionless pseudopressure	$\Psi = \frac{P(r)^2}{P_1^2}$	8.1.7
Dimensionless time	$\tau = \frac{t}{t_0}$	8.1.8
Characteristic time (sec)	$t_0 = \frac{\phi\eta a^2}{kP_1}$	8.1.9
Dimensionless radius	$z = \ln(r/a)$ cylindrical $z = a/r$ spherical	8.1.10
Dimensionless plotting parameter	$\zeta = \frac{(e^z - 1)}{\tau^{1/2}}$ cylindrical $\zeta = \frac{(1/z - 1)}{\tau^{1/2}}$ spherical	8.1.11

Relevant variables are defined in the nomenclature table for section 8 (Table 8-1). The scaling of output to dimensionless space allows us to compare DRSPALL results to different solutions without matching specific input conditions (i.e., values for variables in Table 8-1). As such, selection of input parameter values is not instrumental to proper solution of this test case. Logic is built into the code such that upon activating this test case, the code will:

- calculate the characteristic time  $t_0$  for the particular set of input variables
- calculate dimensional times  $t = t_0\tau$  corresponding to dimensionless times  $\tau = 0.01, 0.1, 1.0, \text{ and } 10.0$

- write to an output ASCII file the following data at  $\tau = 0.01, 0.1, 1.0,$  and  $10.0$ 
  - $t$
  - $\tau$
  - $r, P(r,t), \zeta, \Psi$  ....for ~25 computational cells in the domain starting at the cavity wall

## 8.2 Coalbed Methane Field Scale Test Case

This test case is designed to validate the total spillings solids release model against field observations of coalbed methane cavity completion (“cavitation”) operations. The problem does not include drilling or mud. Only gas plus coal solids flow in the well. Therefore, some special logic is included in the problem setup modules to properly define the problem. The time step algorithm is modified to use the sound speed in gas rather than mud. The wellbore pressure logic uses the mixture equation-of-state, but without the presence of mud and salt.

## 8.3 Internal Logic Checks Test Problem

This test case demonstrates that DRSPALL accurately calculates:

1. Coupling of flows in the wellbore and the repository
2. Tensile failure of homogenous waste material using effective stress and seepage laws
3. Fluidized bed transport of disaggregated waste material
4. Expulsion of disaggregated waste material at the land surface.

There is no special code logic for this test case that affects the calculations. There is coding that creates and formats four ASCII output files that are used in the post-processing of the test case data. The format and content of these files are discussed in VVP/VD for DRSPALL (WIPP PA, 2003a).

## 8.4 Wellbore Hydraulics Model Test Case

The objective of wellbore hydraulics test case is to validate the DRSPALL wellbore calculations against an independent computational fluid dynamics model FLUENT. This

problem is designed to study the wellbore only. As such, the repository domain is decoupled from the wellbore and inactive during execution of the test problem. Input parameters pertaining to the repository are therefore irrelevant in this test case, as are any code output describing repository conditions.

#### ***8.4.1 Lower boundary condition***

The lower boundary to the wellbore domain corresponds to the very bottom of the borehole where repository gases and solids may enter the mud flow stream. In normal DRSPALL execution, the bottomhole pressure acts as a common boundary condition for the inner boundary of the repository and the bottom of the wellbore. Gas and potentially solids are transferred from the repository domain to the wellbore domain at this boundary. For this test case, the lower boundary requires specific control over the mass loading rate of gas and/or solids in order to set up analogous runs with the computational tool FLUENT. These mass loading rates are pre-determined and described in the VVP/VD for DRSPALL (WIPP PA, 2003a). They are implemented in DRSPALL by circumventing the normal coupling function with the repository and building the mass loading directly into the wellbore mass transfer algorithm.

## 9 REFERENCES

- Barree, R.D., Conway, M.W. 1995 "Experimental and Numerical Modeling of Convective Proppant Transport," *Journal of Petroleum Technology*, March, 216-222.
- Belhaj, H.A., K.R. Agha, A.M. Nouri, S.D. Butt, H.F. Vaziri, and M.R. Islam. 2003. "Numerical Simulation of Non-Darcy Flow Utilizing the New Forchheimer's Diffusivity Equation," SPE 81499, presented at the SPE 13<sup>th</sup> Middle East Oil Show & Conference, Bahrain, April, 2003.
- Chan, D.Y.C., Hughes, B.D. and L. Patterson, 1993. *Transient Gas Flow Around Boreholes*, Transport in Porous Media, 10, 137-152. (Copy of document on file in the Sandia WIPP Central Files, Sandia National Laboratories, Albuquerque, NM as WPO#46902.)
- Cherimisinoff, N.P., Cherimisinoff, P.N., 1984. *Hydrodynamics of Gas-Solids Fluidization*, Gulf Publishing Company, Houston, TX, USA.
- Dacun, Li, R.K. Svec, T.W. Engler, and R.B. Grigg,. 2001 "Modeling and Simulation of the Wafer Non-Darcy Flow Experiments," SPE 68822, presented at the SPE Western Regional Meeting, Bakersfield, CA, March 2001.
- Ergun, S. 1952. "Fluid Flow Through Packed Columns," *Chemical Engineering Progress.*, 48(2):89-94.
- Fox, R.W., McDonald, A.T. 1985. *Introduction to Fluid Mechanics, 3<sup>rd</sup> Ed.*, John Wiley and Sons, New York, USA.
- Gross. M.B. and T.W. Thompson. 1998 "Analysis Package for the Semi-Analytical Calculations Conducted In Support of Spalling Release Estimates for the 1998 Annual Sensitivity Study," (ASA98) WPO# 49423, CAO Technical Assistance Contract Carlsbad, New Mexico, for Waste Isolation Pilot Plant (WIPP) Project Sandia National Laboratories Albuquerque, New Mexico.
- Hassanizadeh, S.M. and Gray, W.G. 1987. "High Velocity Flow in Porous Media." *Transport in Porous Media*, vol 2:521-531.
- Hansen, F.D., M.K. Knowles, T.W. Thompson, M. Gross, J.D. McLennan and J.F. Schatz. 1997. *Description and Evaluation of a Mechanistically Based Conceptual Model for Spall*. SAND97-1369. Albuquerque, NM: Sandia National Laboratories.
- Jaeger, J.C. and N.G.W. Cook. 1969. *Fundamentals of Rock Mechanics*, Chapman and Hall Ltd., London, England.
- Lick, W.J. 1989. "Difference Equations from Differential Equations," *Lecture Notes in Engineering*, Springer-Verlag, 1989.
- Li, D., Svec, R.K., Engler, T.W. and Grigg, R.B. 2001. "Modeling and Simulation of the Wafer Non-Darcy Flow Experiments, paper SPE 68822, SPE Western Regional Meeting, Bakersfield, CA, March 26-30.

- Narayanaswamy, G., M.K. Sharma, and G.A. Pope., 1999. "Effect of Heterogeneity on the Non-Darcy Flow Coefficient," *SPE Reservoir Eval. & Eng.* 2 (3) June.
- Oran, E.S., Boris, J.P. 1987. *Numerical Simulation of Reactive Flow*, Elsevier, New York, USA.
- Podio, A.L. and A.P. Yang, 1986. "Well Control Simulator for IBM Personal Computer," IADC/SPE 14737. International Association of Drilling Engineers/Society of Petroleum Engineers paper presented at the IADC/SPE Drilling Conference held in Dallas, TX. February 10-12.
- Press, W.H., B.P. Flannery, S.A. Teukolsky, and W.T. Vetterling, *Numerical Recipes in Pascal —The Art of Scientific Computing*, Cambridge University Press, Cambridge England.
- Rechard, R.P., Gilkey, A.P., Iuzzolino, H.J., Rudeen, D.K., Byle, K.A. 1993. *Programmer's Manual for CAMCON: Compliance Assessment Methodology Controller*. SAND90-1984. Albuquerque, NM: Sandia National Laboratories.
- Serghides, T.K., 1984. "Estimate Friction Factor Accurately," *Chemical Engineering*, March 5, 63-64.
- Timoshenko, S.P. and J.N. Goodier. 1970. *Theory of Elasticity*, Third Ed. McGraw-Hill: New York, NY.
- WIPP PA 1996a, *WIPP PA Users Manual for CAMDAT\_LIB, Version 1.22*, WPO#27727. Albuquerque, NM: Sandia National Laboratories.
- WIPP PA 1996b, *WIPP PA Users Manual for CAMCON\_LIB, Version 2.16*, WPO#27738. Albuquerque, NM: Sandia National Laboratories.
- WIPP PA 1996c, *WIPP PA Users Manual for CAMSUPES\_LIB, Version 2.18*, WPO#27745. Albuquerque, NM: Sandia National Laboratories.
- WIPP PA. 2003a. *Verification and Validation Plan / Validation Document for DRSPALL version 1.00* ERMS# 524782. Carlsbad. NM: Sandia National Laboratories. .
- WIPP PA. 2003b. *Implementation Document for DRSPALL version 1.00*. ERMS# 524781. Carlsbad, NM: Sandia National Laboratories.

## **10 APPENDIX A: FUNCTIONAL REQUIREMENTS**

In general DRSPALL shall calculate the volume of WIPP waste subject to material failure and transport to the surface as a result of an inadvertent drilling intrusion into the repository. More specifically DRSPALL will calculate the following:

- R.1** Compressible, viscous, isothermal, multiphase mixture flow (mud, salt, waste, repository gas) in the wellbore using one dimensional linear geometry and assuming a Newtonian fluid. Either laminar or turbulent flow shall be modeled depending on wellbore and fluid properties.
- R.2** Repository gas flow as single-phase Darcy porous flow using either one dimensional cylindrical or spherical geometry
- R.3** Coupling of the wellbore and the repository flow models prior to and after penetration
- R.4** Spalling (tensile) failure of the homogeneous waste material using an effective stress law with seepage forces
- R.5** Fluidized bed transport of failed (disaggregated) waste material.
- R.6** Mixture expulsion at the surface

### **10.1 External Interface Requirements**

- R.7** DRSPALL shall read an input control file, which may be pre-generated using a text processor. It will contain numerical control parameters and, optionally, material properties and problem geometry.
- R.8** Properties and non-numerical control parameters will, optionally, be read from a CDB.
- R.9** Grid, properties, parameters and spatial and time dependent results will be written to an output CDB.

DRSPALL will link to the standard WIPP code libraries, namely, CAMDAT\_LIB, CAMCON\_LIB, and CAMSUPES\_LIB (Rechard et al., 1993). User interactions will consist of command line execution, batch files, and input files.